# Supporting Information for

# At-a-site and between-site variability of bedload transport, inferred from continuous surrogate monitoring, and comparison to predictive equations

Dieter Rickenmann 1,2

<sup>1</sup>Swiss Federal Research Institute WSL, Birmensdorf, 8903, Switzerland

### **Contents of this file**

Tables S1 to S6

Figures S1 to S31

Table S1. Exponents  $m_{\text{tot}}$ ,  $m_{\text{red}}$  and dimensionless reference shear stresses  $\tau^*_{\text{rD50}}$ ,  $\tau^{*\prime}_{\text{rD50}}$  derived from analysis of temporal variation of bedload transport relation for phase-2 transport conditions.

iporai variatioi	i di bedidad ti	ansport	elation for	i for phase-2 transport cor				
		W*tot	analysis	W*red analysis				
year(s)	no. time windows	m <sub>tot</sub>	$ au^*_{ ext{rD50}}$	m <sub>red</sub>	τ*′ <sub>rD50</sub>			
2016	5 double-	weeks						
		12.62	0.039	8.47	0.025			
		15.30	0.042	10.47	0.028			
		14.04	0.042	9.39	0.028			
		13.75	0.043	9.38	0.029			
		12.43	0.037	8.05	0.022			
	mean	13.63	0.040	9.15	0.026			
2011	9 double-ı	weeks						
		5.03	0.076	2.01	0.010			
		6.27	0.092	2.64	0.020			
		5.97	0.099	2.53	0.023			
		9.70	0.100	4.59	0.029			
		7.30	0.093	3.28	0.022			
		6.92	0.101	3.07	0.026			
		7.61	0.118	3.41	0.039			
		3.59	0.123	1.26	0.024			
		7.16	0.080	3.06	0.015			
	mean	6.62	0.098	2.87	0.023			
2019	10 double-	weeks						
		10.54	0.115	3.94	0.017			
		5.38	0.103	1.61	0.005			
		12.03	0.116	4.61	0.018			
		17.02	0.112	6.87	0.019			
		10.73	0.115	4.03	0.017			
		16.10	0.097	6.45	0.013			
	year(s)  2016  2011	year(s) no. time windows  2016 5 double-to  mean  2011 9 double-to  mean	W*tot   Work   Windows   Windows	year(s)         no. time windows         mtot windows         t*rp50           2016         5 double-weeks         12.62         0.039           15.30         0.042         14.04         0.042           13.75         0.043         12.43         0.037           mean         13.63         0.040           2011         9 double-weeks         5.03         0.076           6.27         0.092         5.97         0.099           9.70         0.100         7.30         0.093           6.92         0.101         7.61         0.118           3.59         0.123         7.16         0.080           mean         6.62         0.098           2019         10 double-weeks         10.54         0.115           5.38         0.103         12.03         0.116           17.02         0.112         10.73         0.115	year(s)         no. time windows         mtot         \tau^*_{rD50}         m_{red}           2016         5 double-weeks         12.62         0.039         8.47           15.30         0.042         10.47           14.04         0.042         9.39           13.75         0.043         9.38           12.43         0.037         8.05           mean         13.63         0.040         9.15           2011         9 double-weeks         9.15           2011         9 double-weeks         2.01           6.27         0.092         2.64           5.97         0.099         2.53           9.70         0.100         4.59           7.30         0.093         3.28           6.92         0.101         3.07           7.61         0.118         3.41           3.59         0.123         1.26           7.16         0.080         3.06           mean         6.62         0.098         2.87           2019         10 double-weeks         10.54         0.115         3.94           5.38         0.103         1.61         12.03         0.116         4.61 <tr< td=""></tr<>			

<sup>&</sup>lt;sup>2</sup>FluvialTech GmbH, Zürich, 8052, Switzerland

AV_dw			14.56	0.113	5.76	0.018
AV_dw			14.00	0.115	5.50	0.019
AV_dw			13.34	0.123	5.20	0.022
VN_dw			5.71	0.198	1.76	0.049
		mean	11.94	0.121	4.57	0.020
Erlenbach A	1986-1999	7 sub-pe	eriods			
EB_pid_A			10.98	0.175	5.87	0.028
EB_pid_A			11.33	0.174	6.14	0.028
EB_pid_A			10.58	0.174	5.70	0.028
EB_pid_A			11.18	0.174	6.02	0.028
EB_pid_A			11.70	0.177	6.15	0.029
EB_pid_A			11.03	0.175	5.91	0.028
EB_pid_A			10.06	0.172	5.48	0.027
		mean	10.98	0.174	5.90	0.028
Erlenbach B	2002-2016	6 sub-pe	eriods			
EB_pid_B			8.23	0.159	4.82	0.025
EB_pid_B			11.02	0.176	5.87	0.029
EB_pid_B			11.32	0.176	6.02	0.029
EB_pid_B			10.92	0.175	5.82	0.028
EB_pid_B			9.66	0.169	5.36	0.027
EB_pid_B			13.36	0.179	6.82	0.029
		mean	10.75	0.172	5.79	0.028
For comparison,	data from Schne	eider et al. (201	!5a)			
SEA_SS	14 streams	mean	17.86	0.099	8.47	0.036
SEA_HS	21 streams	mean	7.51	0.037	5.15	0.028
	1	1				

Table S2. Albula. Mean ratios of calculated to observed bedload masses for period A and for period B, and results of cumulative sum analysis. Table includes begin and end date of yearly observation period, and squared correlation coefficient R2 for a linear model (LM) fitted to the function CumSum ( $Q_{bx}$ ) vs. CumSum ( $Q_{bM}$ ), determined for values ordered according to increasing Q ("incQ") and for  $\tau^*_{D50} => 1.1 \ \tau^*_{rD50} (Q_1.1)$ .

Period (year)	minutes	rt_year	rt_incQ	R2 for LM	rt within factor 3 from X minutes	rr_year	rr_incQ	R2 for LM	rr within factor 3 from X minutes	Qmax (m3/s)	Qmax / Q_1.1
13.05. – 10.09.2016	78761	0.570	0.614	0.969	33000	0.442	0.453	0.978	25000	92.02	4.30
18.05. – 10.08.2017	24668	0.108	0.294	0.962	16000	0.132	0.255	0.998	9000	29.20	1.36
23.04. – 31.10.2018	36888	0.253	0.251	0.989	3200	0.224	0.210	0.991	2100	44.22	2.07
02.06. – 31.10.2019	44633	0.907	0.796	0.991	5700	0.670	0.597	0.993	5600	108.30	5.06
11.05. – 10.10.2020	39952	0.230	0.336	0.920	29000	0.185	0.264	0.931	29000	54.48	2.55
10.05. – 20.06.2021	27076	0.162	0.218	0.926	19000	0.134	0.177	0.936	18000	40.56	1.90
01.01. – 31.12.2022	22171	0.035	0.260	0.999	NA	0.067	0.243	0.997	NA	24.39	1.14
13.05. – 25.10.2023	43890	0.584	0.910	0.992	37000	0.428	0.663	0.993	37000	84.80	3.96
Mean		0.356	0.460		20414	0.285	0.358		17957		

Table S3. Navisence. Mean ratios of calculated to observed bedload masses for period A and for period B, and results of cumulative sum analysis. Table includes begin and end date of yearly observation period, and squared correlation coefficient R2 for a linear model (LM) fitted to the function CumSum ( $Q_{\rm bx}$ ) vs. CumSum ( $Q_{\rm bM}$ ), determined for values ordered according to increasing Q ("incQ") and for  $\tau^*_{\rm D50}$  => 1.1  $\tau^*_{\rm rD50}$  ( $Q_{\rm L}$ 1.1).

V 1030 (~	-,-										
Period (year)	minutes	rt_year	rt_incQ	R2 for LM	rt within factor 3 from X minutes	rr_year	rr_incQ	R2 for LM	rr within factor 3 from X minutes	Qmax (m3/s)	Qmax / Q_1.1
18.05. – 30.09.2011	186439	0.066	1.575	0.801	NA	0.437	5.724	0.861	NA	30.69	1.65
01.05. – 30.09.2012	220319	0.049	0.590	0.876	NA	0.630	2.949	0.932	NA	23.10	1.24
01.05. – 07.08.2013	142384	0.461	0.704	0.988	(73000)	2.991	2.653	0.997	73000	33.23	1.79
18.07. – 30.09.2019	66436	0.490	1.423	0.915	32000	3.055	5.430	0.956	25000	34.44	1.85
02.05. – 30.09.2020	117214	0.384	1.914	0.995	NA	3.002	8.468	0.999	57000	27.41	1.47
10.05. – 30.09.2021	105612	0.879	3.067	0.983	(24000)	7.043	14.500	0.996	19000	26.92	1.45
Mean		0.388	1.546		32000	2.860	6.621		43500		

Table S4. Avançon. Mean ratios of calculated to observed bedload masses for period A and for period B, and results of cumulative sum analysis. Table includes begin and end date of yearly observation period, and squared correlation coefficient R2 for a linear model (LM) fitted to the function CumSum ( $Q_{\rm bx}$ ) vs. CumSum ( $Q_{\rm bM}$ ), determined for values ordered according to increasing Q ("incQ") and for  $\tau^*_{\rm D50}$  => 1.1  $\tau^*_{\rm rD50}$  ( $Q_{\rm L}$ 1.1).

₹ 1D30 (¬_===											
Period	minutes	rt_year	rt_incQ	R2	rt within	rr_year	rr_incQ	R2	rr within	Qmax	Qmax /
(year)				for	factor 3			for	factor 3	(m3/s)	Q_1.1
				LM	from X			LM	from X		
					minutes				minutes		
16.04. –	139106	5.663	8.135	0.996	28000	0.882	0.973	0.979	30000	6.88	4.74
29.10.2018											
17.04. –	146560	5.221	6.287	0.830	23000	1.460	1.459	0.704	25000	6.14	4.23
31.10.2019											
14.04. –	90302	3.593	6.588	0.990	16000	0.386	0.577	0.937	20000	4.66	3.21
30.08.2020											
25.04. –	23608	5.875	7.389	0.979	4700	0.588	0.700	0.906	5000	2.79	1.92
26.09.2021											
10.05. –	37562	4.633	4.793	0.292	6700	1.954	1.519	0.694	16000	6.90	4.76
31.10.2022											
18.04. –	95707	11.346	14.420	0.985	91	2.820	2.436	0.853	216	6.86	4.73
30.10.2023											
Mean		6.055	7.935		13082	1.349	1.277		16036		

Table S5. Erlenbach. Mean ratios of calculated to observed bedload masses for period A and for period B, and results of cumulative sum analysis. Table includes begin and end date of yearly observation period, and squared correlation coefficient R2 for a linear model (LM) fitted to the function CumSum ( $Q_{\rm bx}$ ) vs. CumSum ( $Q_{\rm bm}$ ), determined for values ordered according to increasing Q ("incQ") and for  $\tau^*_{\rm D50}$  => 1.1  $\tau^*_{\rm rD50}$  ( $Q_{\rm L}$ 1.1).

· 1030 (~/											
Period (year)	minutes	rt_year	rt_incQ	R2 for	rt within	rr_year	rr_incQ	R2 for	rr within	Qmax	Qmax /
				LM	factor 3			LM	factor 3	(m3/s)	Q_1.1
					from X				from X		
					minutes				minutes		
20.10.1986 -	37930	0.840	0.994	0.969	0	0.248	0.163	0.916	3100	9.80	14.83
30.09.1999											
16.11.2002 -	33917	0.817	0.940	0.980	3800	0.343	0.218	0.870	4700	15.60	23.60
26.10.2016											
Mean		0.829	0.967		1900	0.295	0.191		3900		

### Q<sub>b</sub> vs. Q plots for the Albula

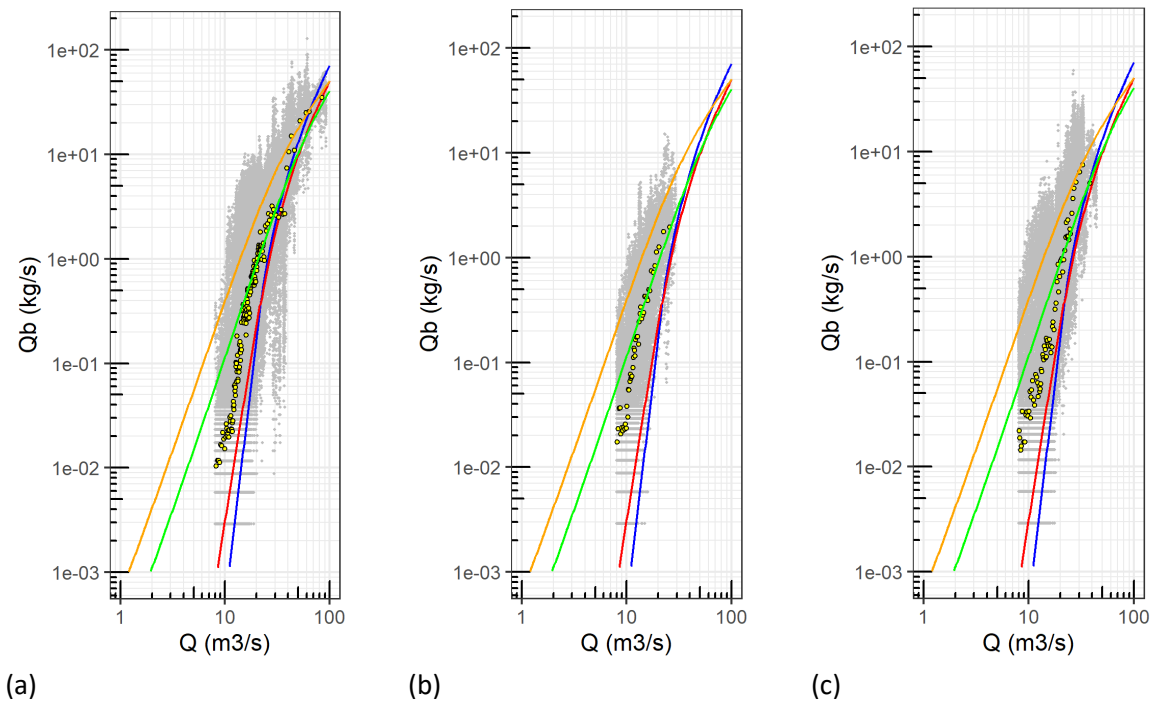


Figure S1. Albula,  $Q_b$  vs. Q plots with 4 bedload equations, for (a) 2016, (b) 2017, (c) 2018. The legend is the same as in Figure 3 of the paper. The binned geometric mean values of  $Q_b$  for binned Q classes were determined by setting zero  $Q_b$  values to  $Q_b$  = 1e-4 kg/s, to match the  $Q_{bM\ binned}$  values for the Albula 2016 in Figure 3.

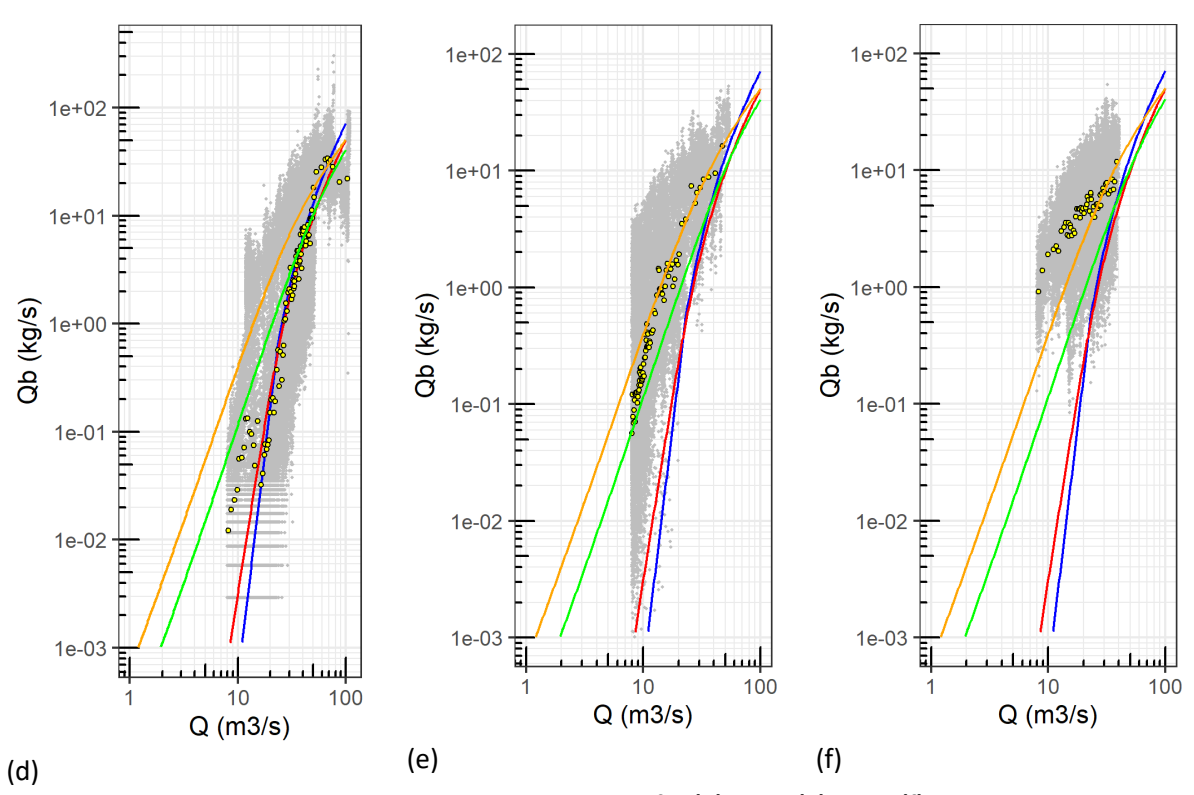


Figure S2. Albula,  $Q_b$  vs. Q plots with 4 bedload equations, for (d) 2019, (e) 2020, (f) 2021. The legend is the same as in Figure 3 of the paper. The binned geometric mean values of  $Q_b$  for binned Q classes were determined by setting zero  $Q_b$  values to  $Q_b$  = 1e-4 kg/s, to match the  $Q_{bM\ binned}$  values for the Albula 2016 in Figure 3.

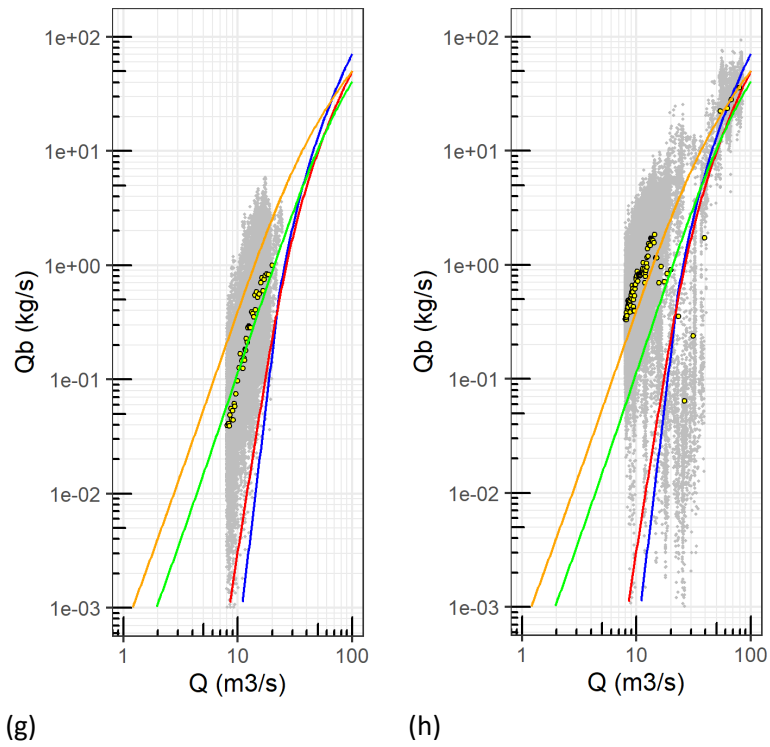
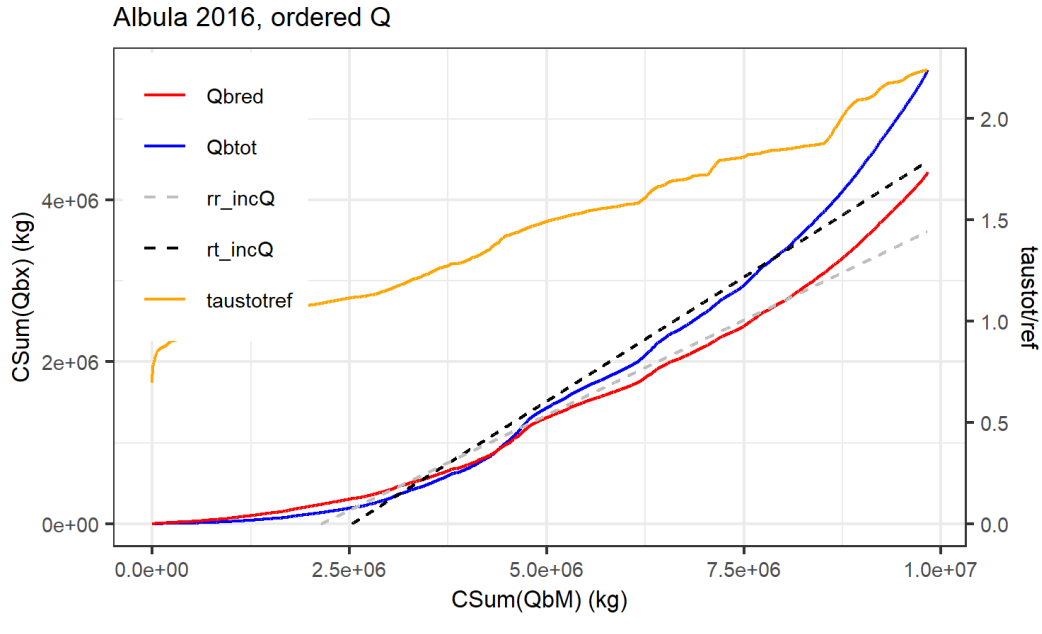


Figure S3. Albula,  $Q_b$  vs. Q plots with 4 bedload equations, (g) 2022, (h) 2023. The legend is the same as in Figure 3 of the paper. The binned geometric mean values of  $Q_b$  for binned Q classes were determined by setting zero  $Q_b$  values to  $Q_b$  = 1e-4 kg/s, to match the  $Q_{bM\ binned}$  values for the Albula 2016 in Figure 3.

### **CumSum analysis for the Albula**



(a)

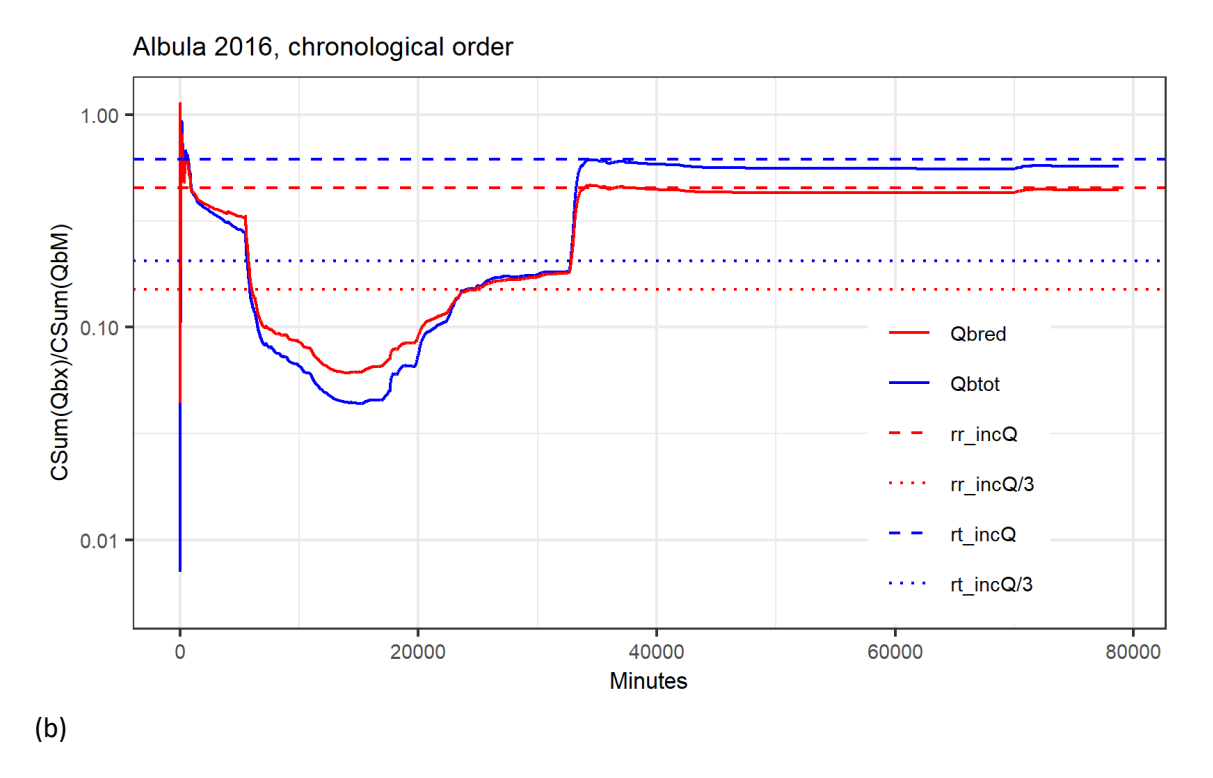
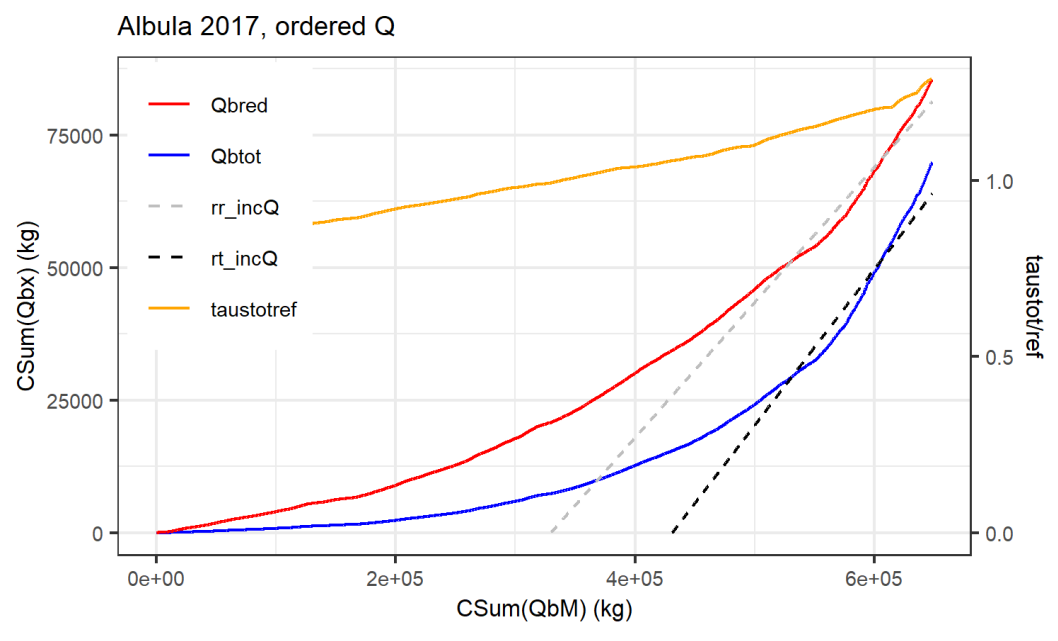


Figure S4. Albula, summer 2016. (a) Application of a liner model (gray and black dashed lines) for the cumulative sum of calculated (SumQbx) vs. measured (SumQbM) bedload masses; values are ordered according to increasing discharge Q. (b) Ratio of cumulative sum of calculated (CSum(Qbx)) to cumulative sum of observed (CSum(QbM)) bedload masses vs. time (in minutes); values are in chronological order.



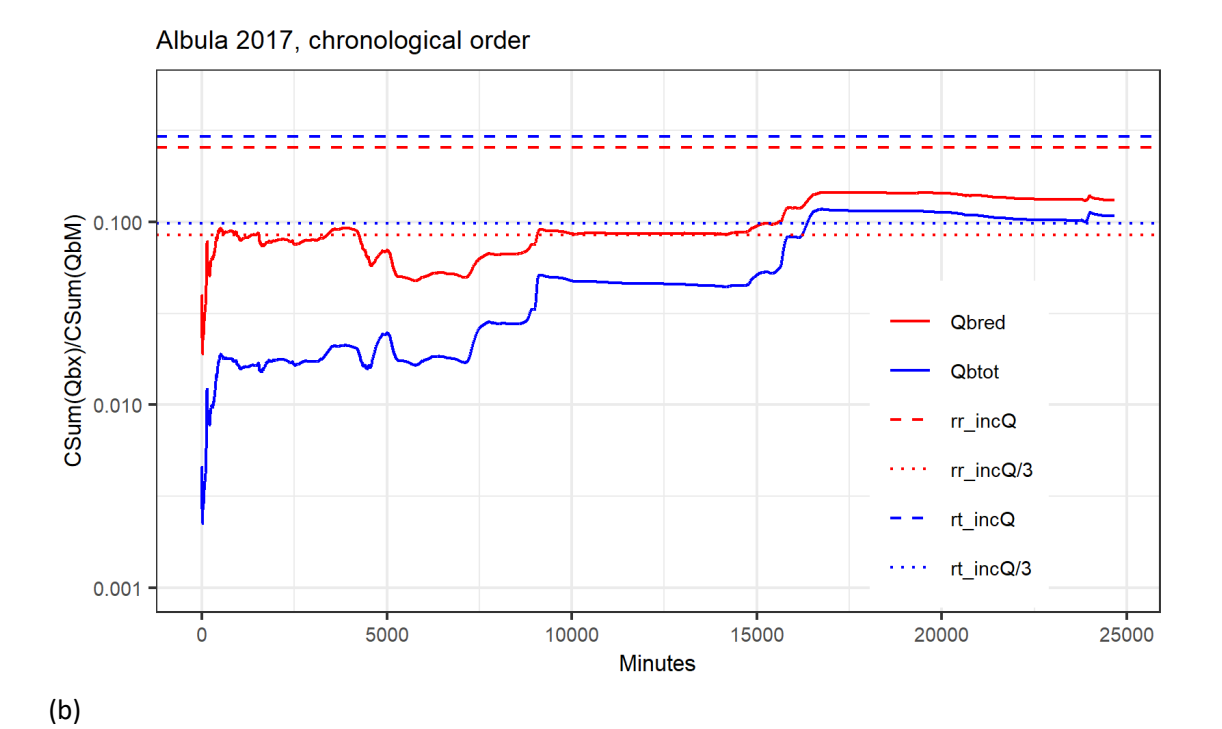
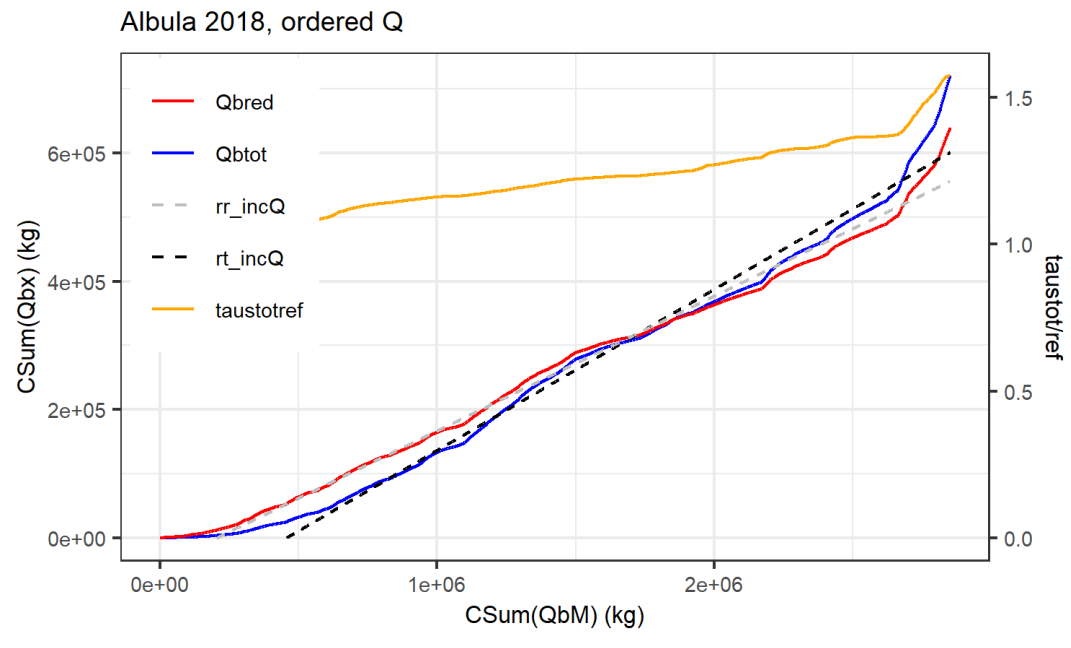


Figure S5. Albula, summer 2017. (a) Application of a liner model (gray and black dashed lines) for the cumulative sum of calculated (SumQbx) vs. measured (SumQbM) bedload masses; values are ordered according to increasing discharge Q. (b) Ratio of cumulative sum of calculated (CSum(Qbx)) to cumulative sum of observed (CSum(QbM)) bedload masses vs. time (in minutes); values are in chronological order.



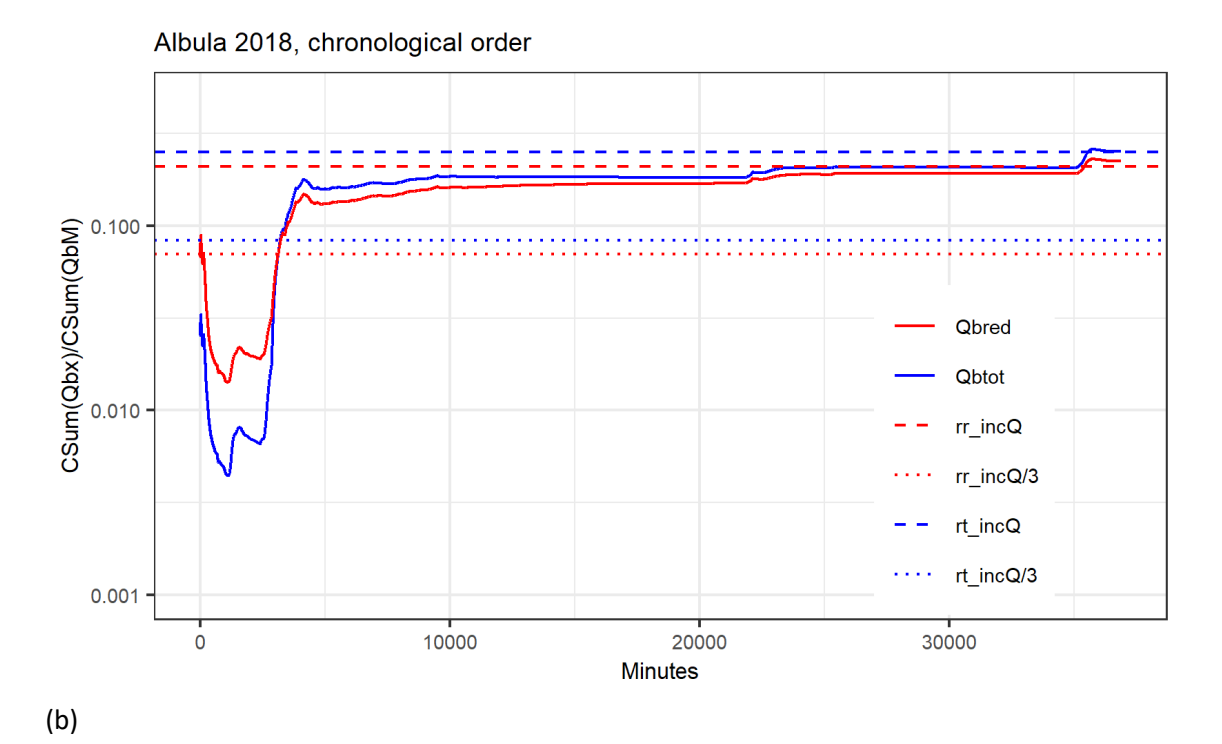
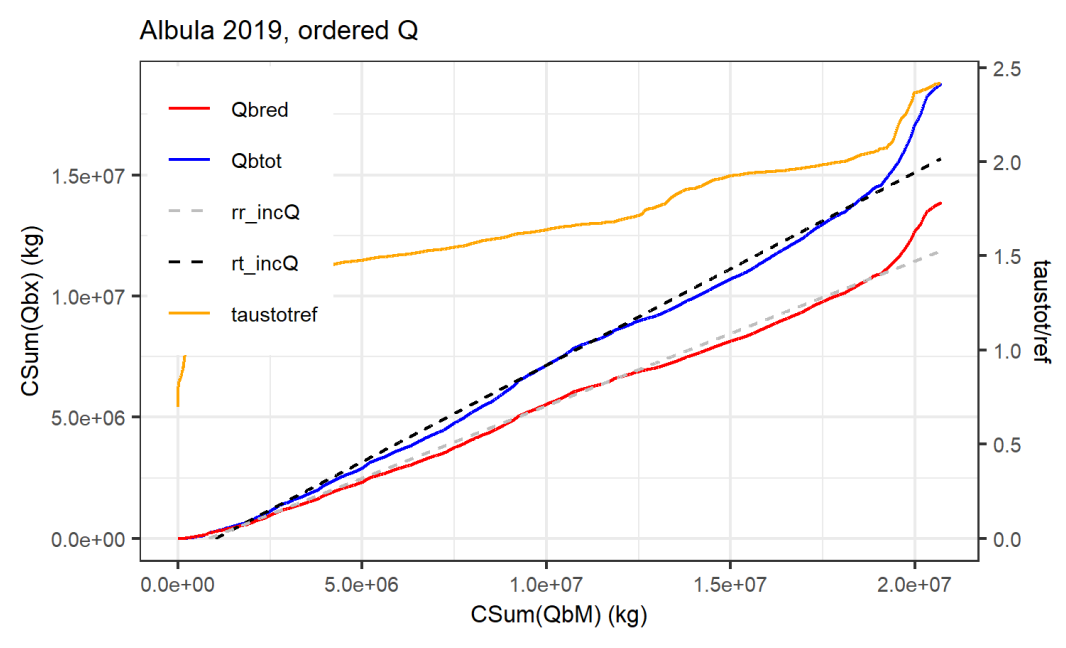


Figure S6. Albula, summer 2018. (a) Application of a liner model (gray and black dashed lines) for the cumulative sum of calculated (SumQbx) vs. measured (SumQbM) bedload masses; values are ordered according to increasing discharge Q. (b) Ratio of cumulative sum of calculated (CSum(Qbx)) to cumulative sum of observed (CSum(QbM)) bedload masses vs. time (in minutes); values are in chronological order.



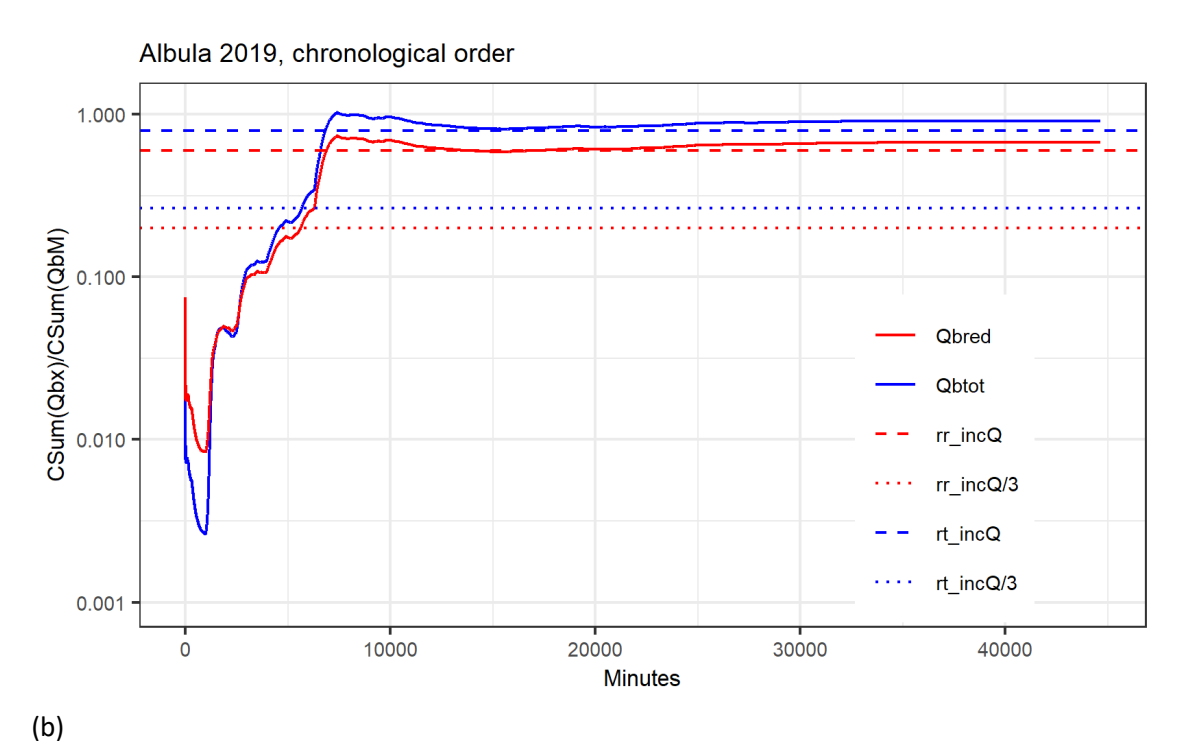
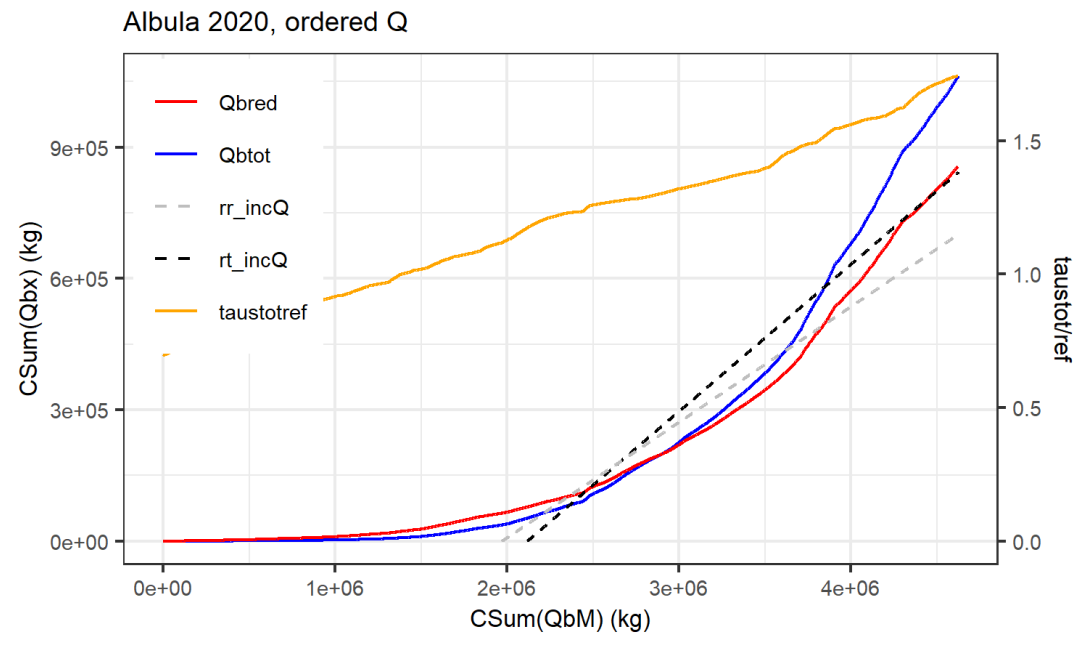


Figure S7. Albula, summer 2019. (a) Application of a liner model (gray and black dashed lines) for the cumulative sum of calculated (SumQbx) vs. measured (SumQbM) bedload masses; values are ordered according to increasing discharge Q. (b) Ratio of cumulative sum of calculated (CSum(Qbx)) to cumulative sum of observed (CSum(QbM)) bedload masses vs. time (in minutes); values are in chronological order.



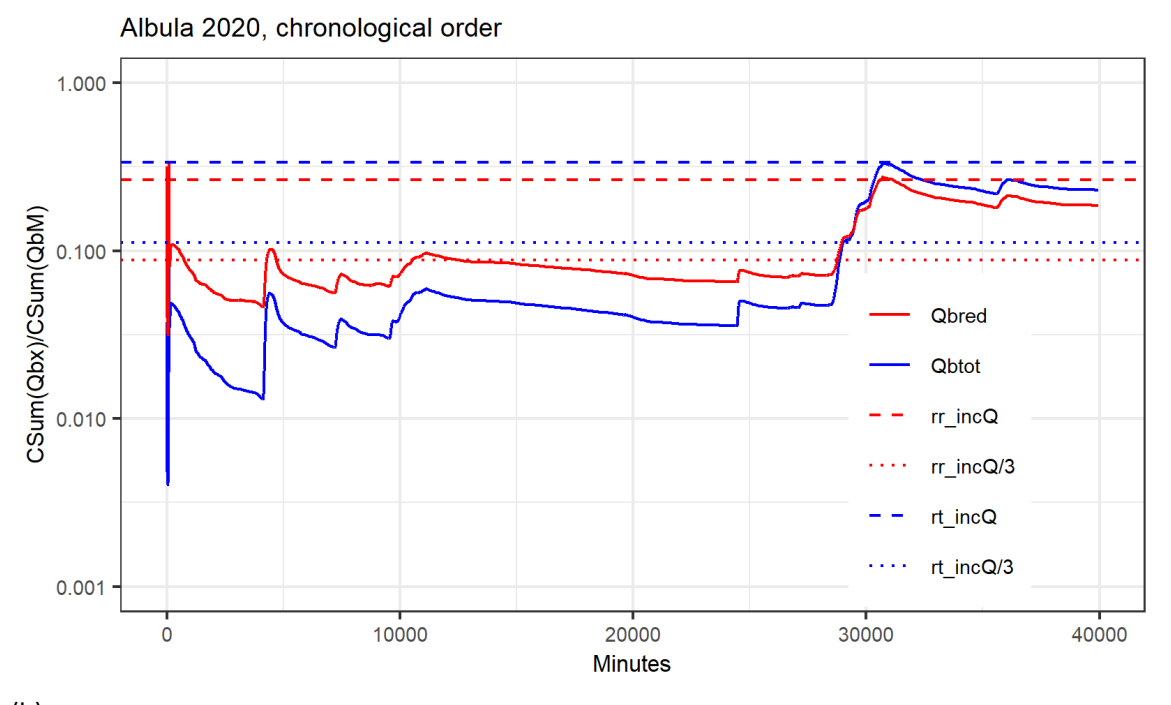
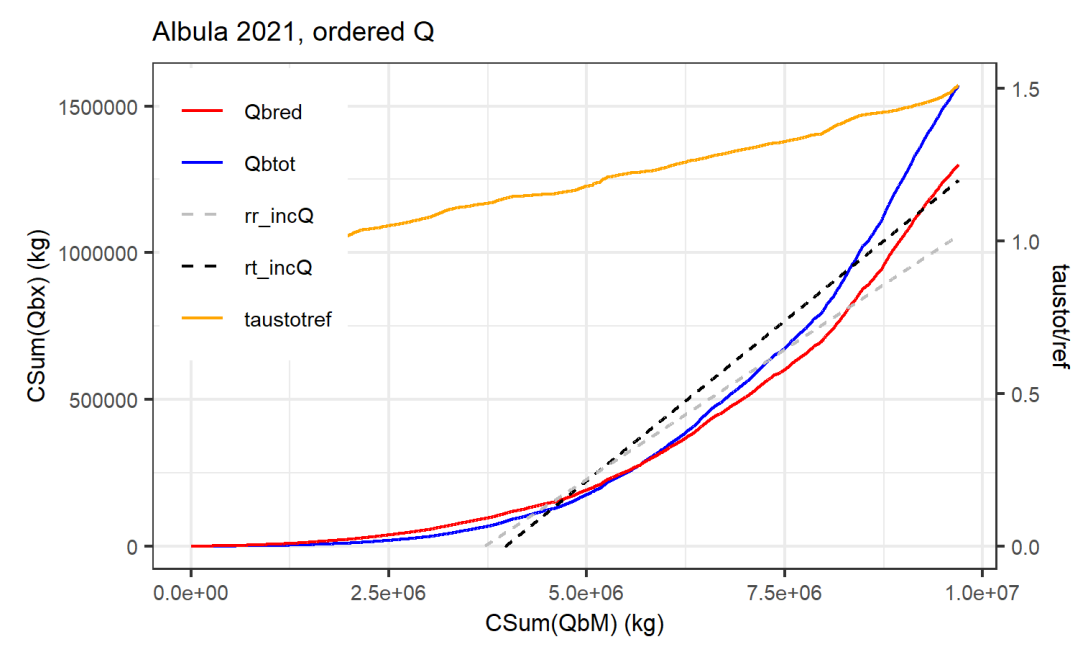


Figure S8. Albula, summer 2020. (a) Application of a liner model (gray and black dashed lines) for the cumulative sum of calculated (SumQbx) vs. measured (SumQbM) bedload masses; values are ordered according to increasing discharge Q. (b) Ratio of cumulative sum of calculated (CSum(Qbx)) to cumulative sum of observed (CSum(QbM)) bedload masses vs. time (in minutes); values are in chronological order.



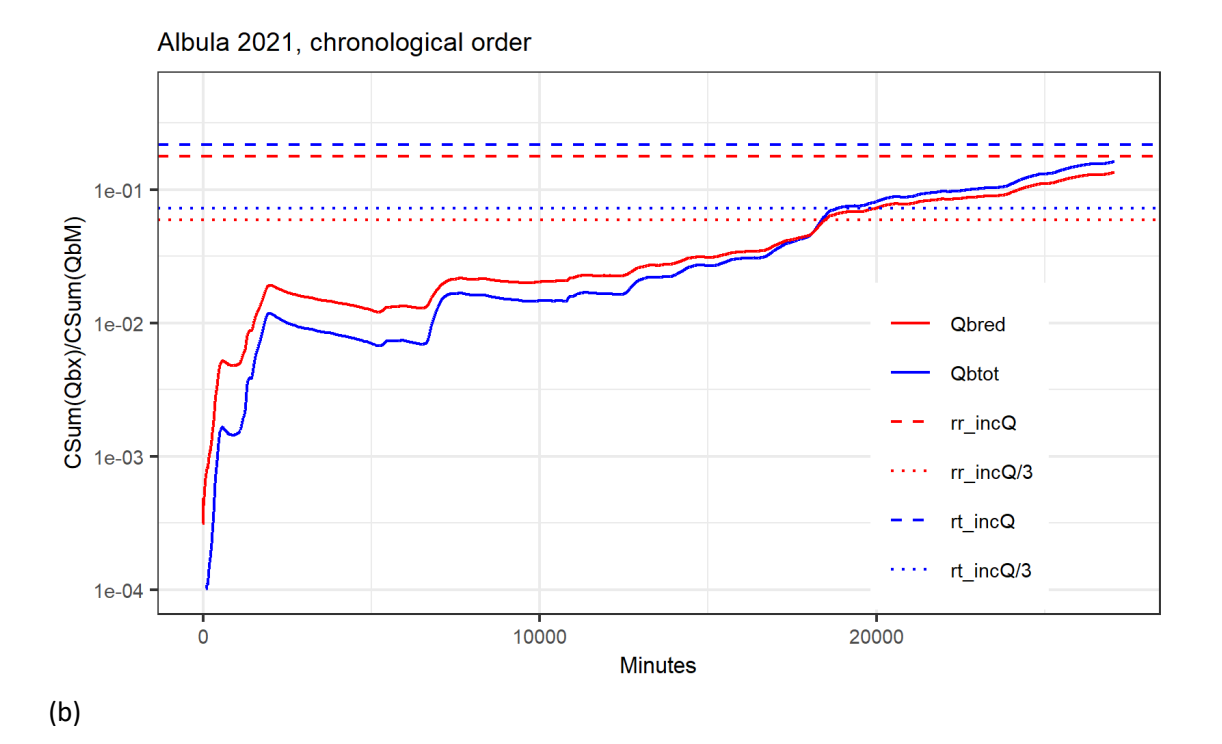
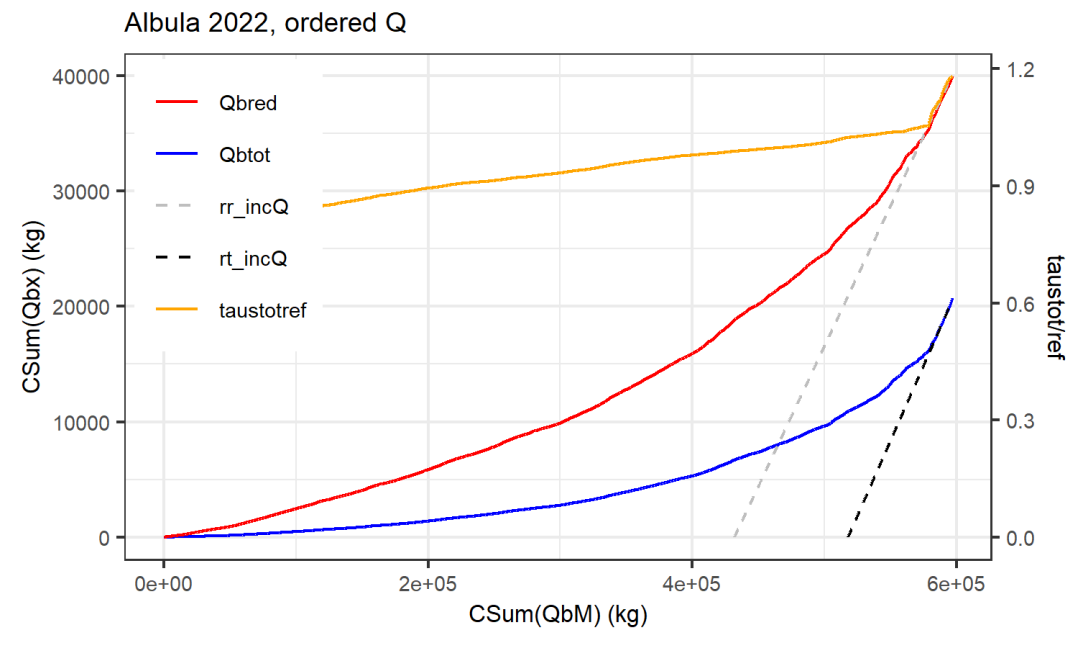


Figure S9. Albula, summer 2021. (a) Application of a liner model (gray and black dashed lines) for the cumulative sum of calculated (SumQbx) vs. measured (SumQbM) bedload masses; values are ordered according to increasing discharge Q. (b) Ratio of cumulative sum of calculated (CSum(Qbx)) to cumulative sum of observed (CSum(QbM)) bedload masses vs. time (in minutes); values are in chronological order.



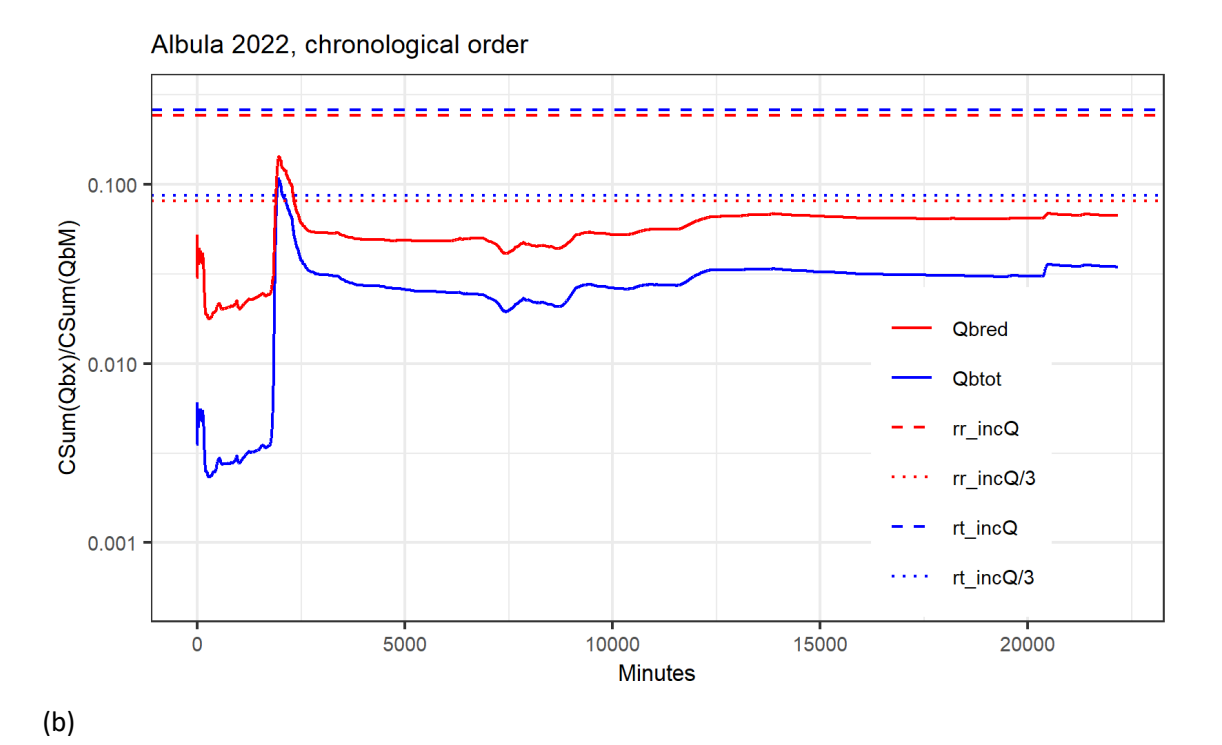
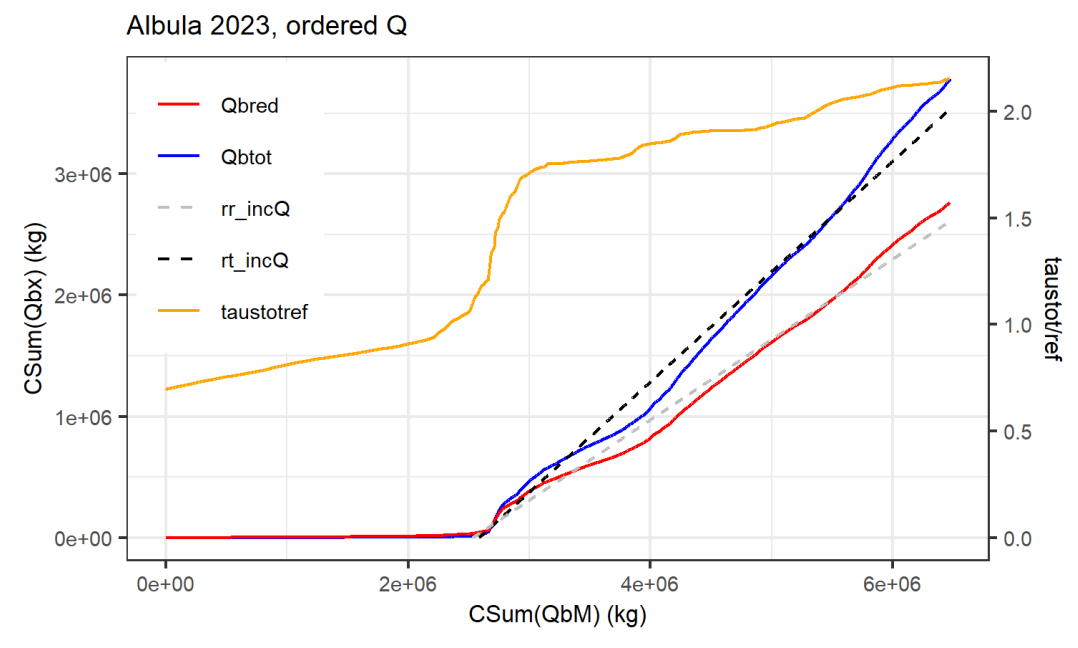


Figure S10. Albula, summer 2022. (a) Application of a liner model (gray and black dashed lines) for the cumulative sum of calculated (SumQbx) vs. measured (SumQbM) bedload masses; values are ordered according to increasing discharge Q. (b) Ratio of cumulative sum of calculated (CSum(Qbx)) to cumulative sum of observed (CSum(QbM)) bedload masses vs. time (in minutes); values are in chronological order.



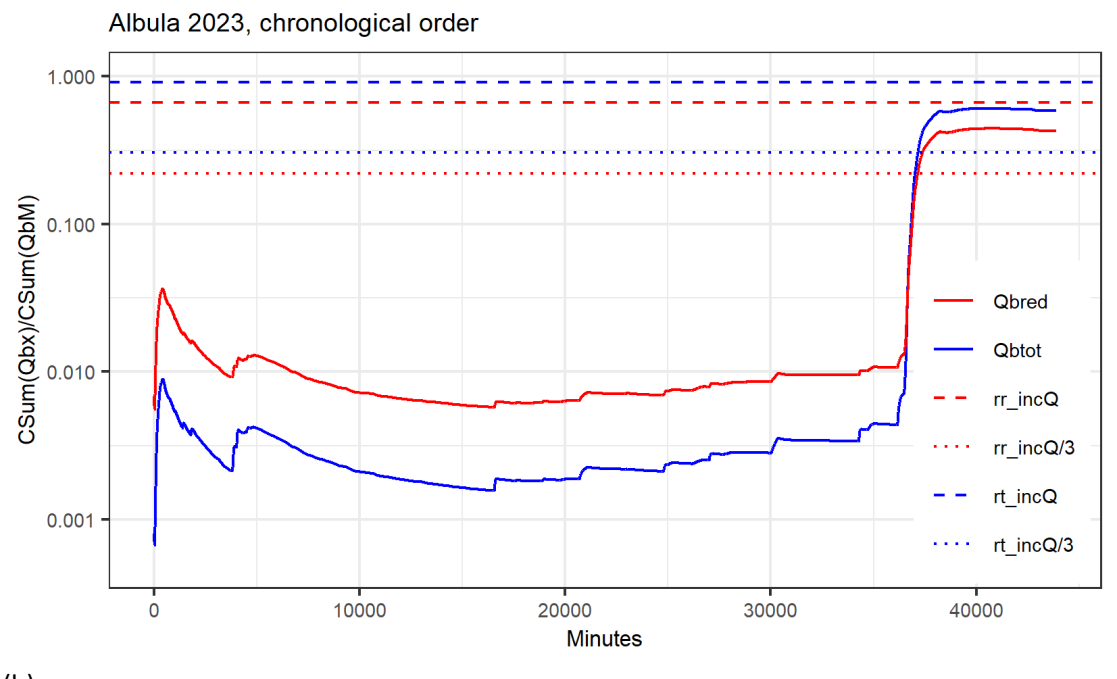


Figure S11. Albula, summer 2023. (a) Application of a liner model (gray and black dashed lines) for the cumulative sum of calculated (SumQbx) vs. measured (SumQbM) bedload masses; values are ordered according to increasing discharge Q. (b) Ratio of cumulative sum of calculated (CSum(Qbx)) to cumulative sum of observed (CSum(QbM)) bedload masses vs. time (in minutes); values are in chronological order.

# Q<sub>b</sub> vs. Q plots for the Navisence

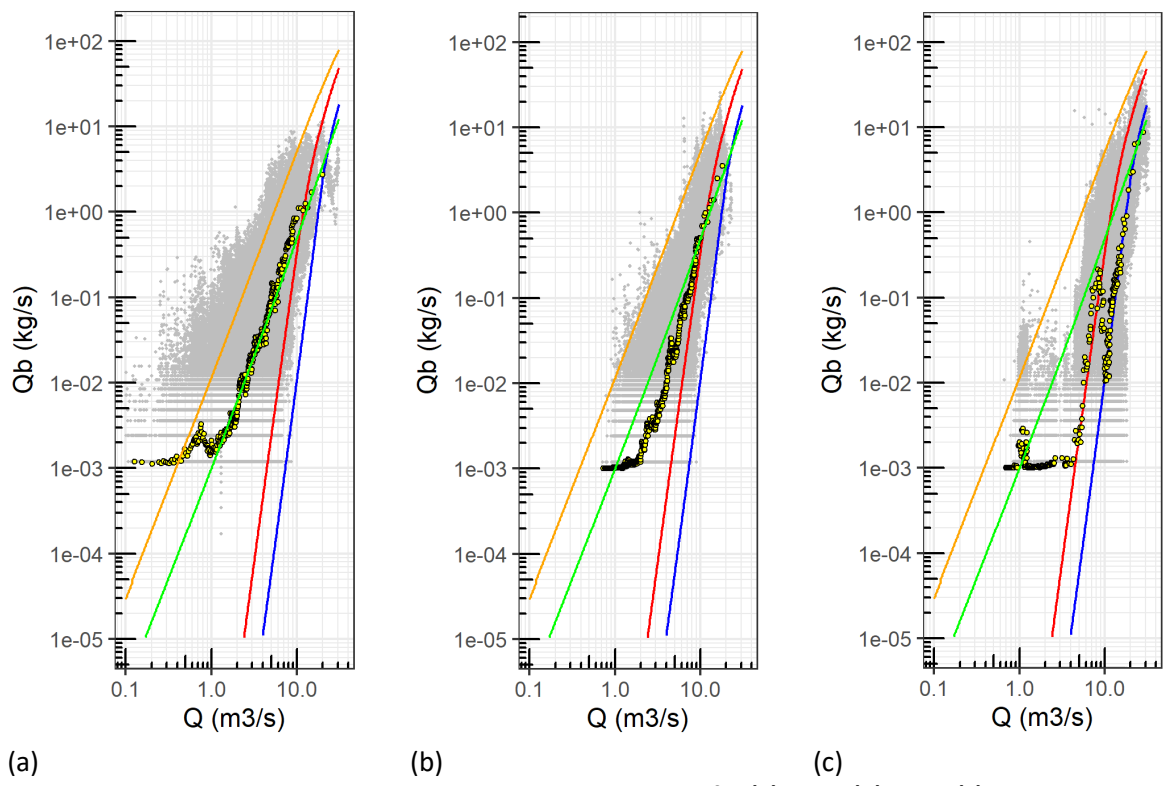


Figure S12. Navisence,  $Q_b$  vs. Q plots with 4 bedload equations, for (a) 2011, (b) 2012, (c) 2013. The legend is the same as in Figure 3 of the paper. The binned geometric mean values of  $Q_b$  for binned Q classes were determined by setting zero  $Q_b$  values to  $Q_b$  = 1e-3 kg/s, to match the  $Q_{bM\ binned}$  values for the Navisence 2011 in Figure 3.

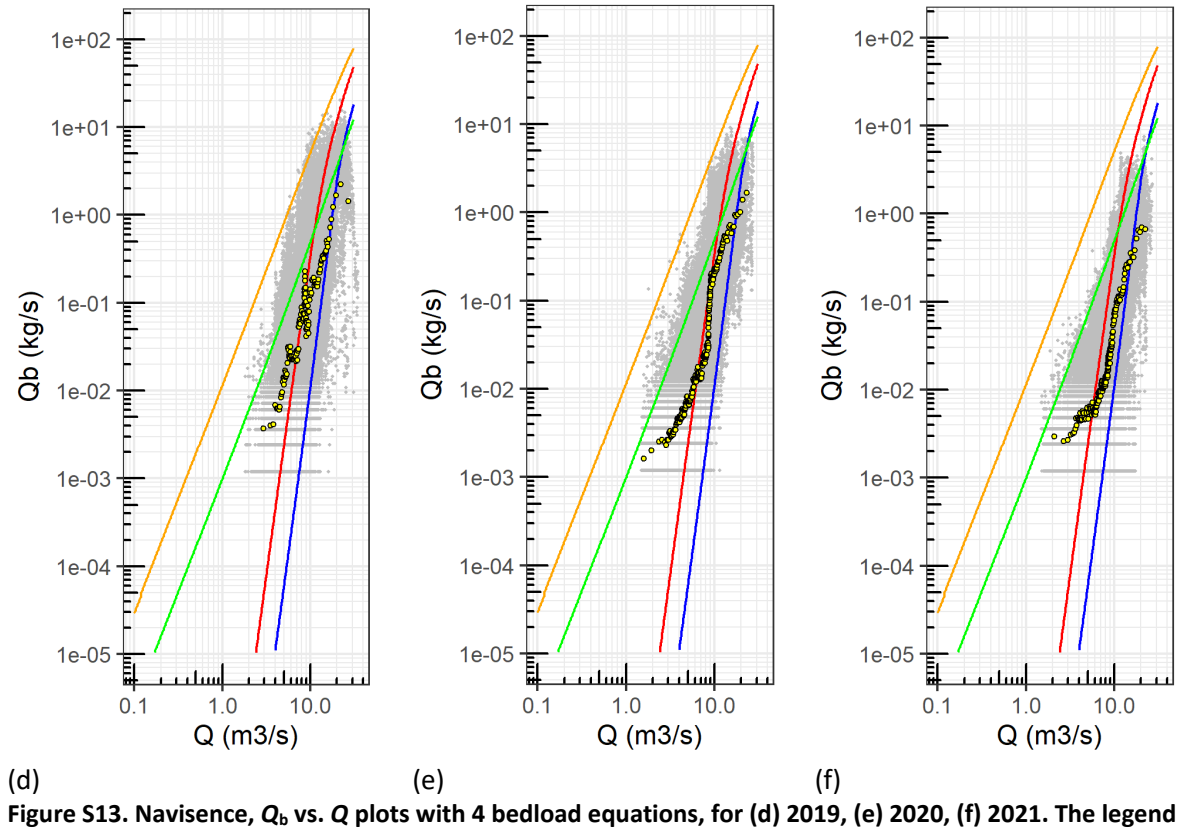


Figure S13. Navisence,  $Q_b$  vs. Q plots with 4 bedload equations, for (d) 2019, (e) 2020, (f) 2021. The legend is the same as in Figure 3 of the paper. The binned geometric mean values of  $Q_b$  for binned  $Q_b$  classes were determined by setting zero  $Q_b$  values to  $Q_b = 1e-3$  kg/s, to match the  $Q_{bM \ binned}$  values for the Navisence 2011 in Figure 3.

# **CumSum analysis for the Navisence**

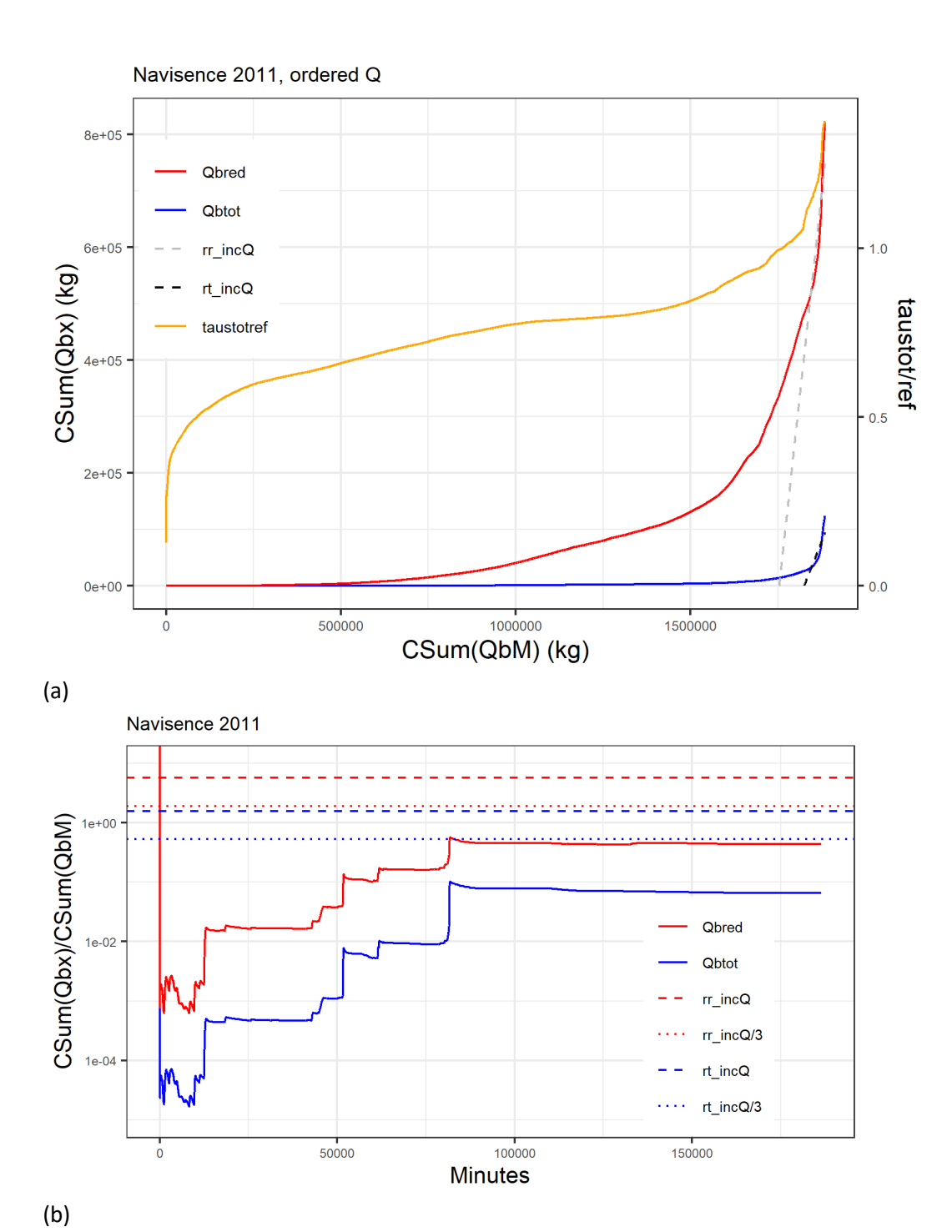
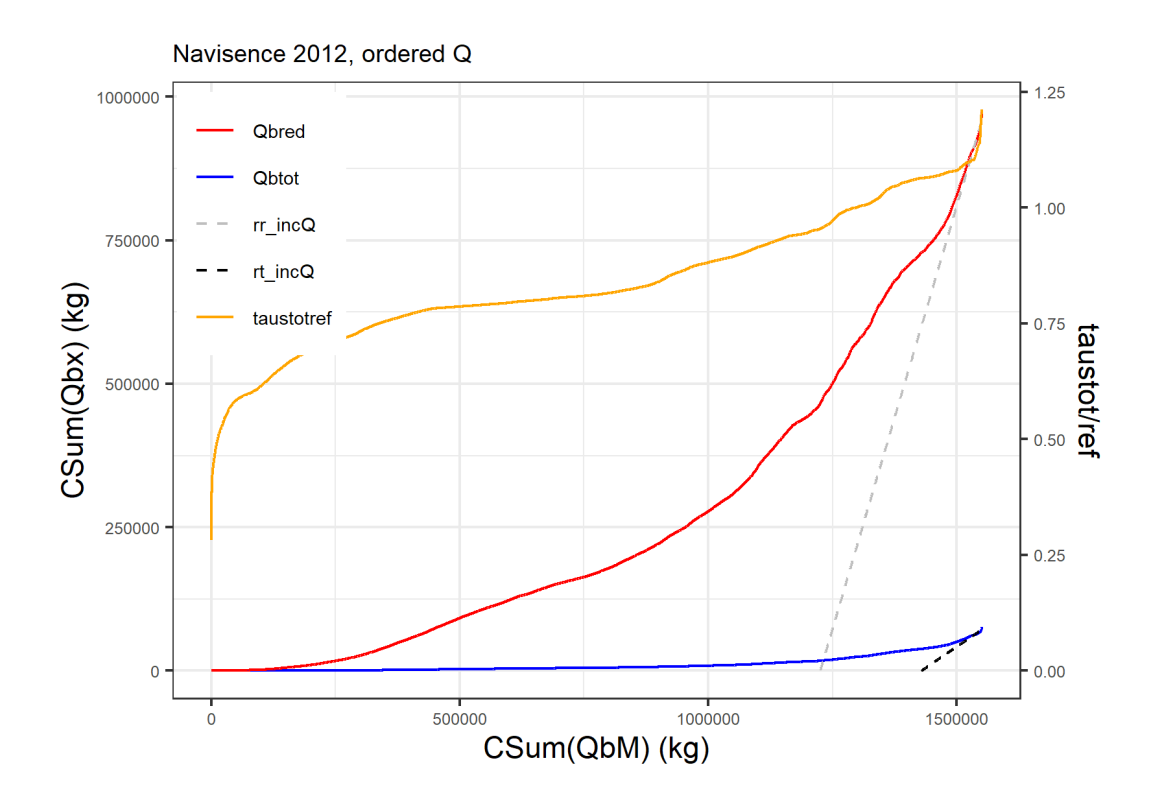


Figure S14. Navisence, summer 2011. (a) Application of a liner model (gray and black dashed lines) for the cumulative sum of calculated (SumQbx) vs. measured (SumQbM) bedload masses; values are ordered according to increasing discharge Q. (b) Ratio of cumulative sum of calculated (CSum(Qbx)) to cumulative sum of observed (CSum(QbM)) bedload masses vs. time (in minutes); values are in chronological order.



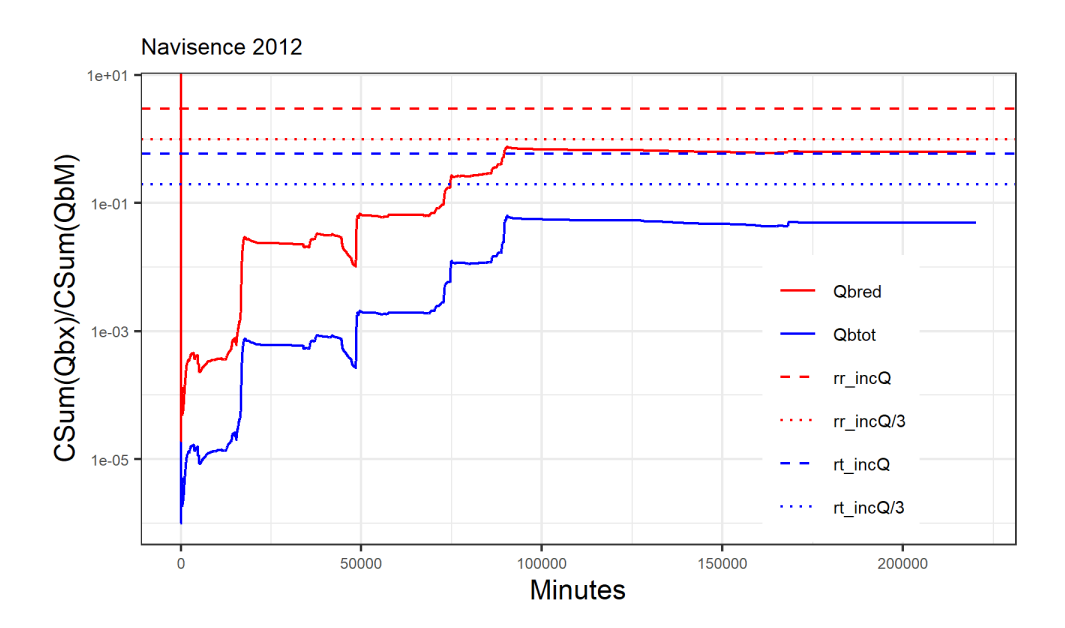
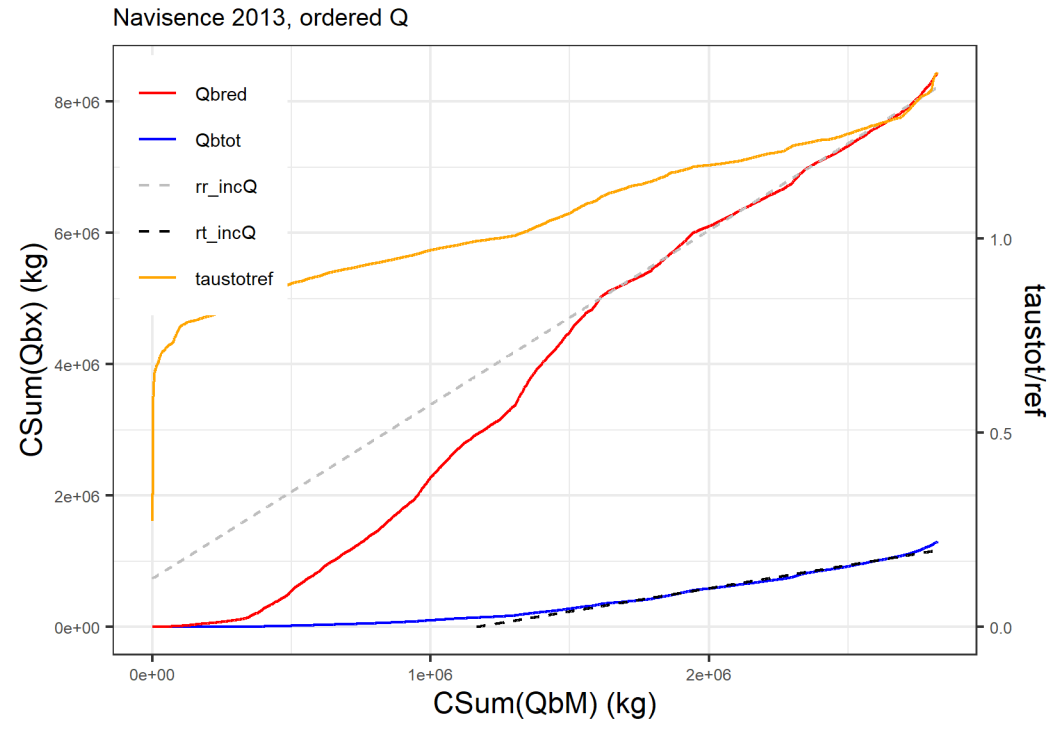


Figure S15. Navisence, summer 2012. (a) Application of a liner model (gray and black dashed lines) for the cumulative sum of calculated (SumQbx) vs. measured (SumQbM) bedload masses; values are ordered according to increasing discharge Q. (b) Ratio of cumulative sum of calculated (CSum(Qbx)) to cumulative sum of observed (CSum(QbM)) bedload masses vs. time (in minutes); values are in chronological order.



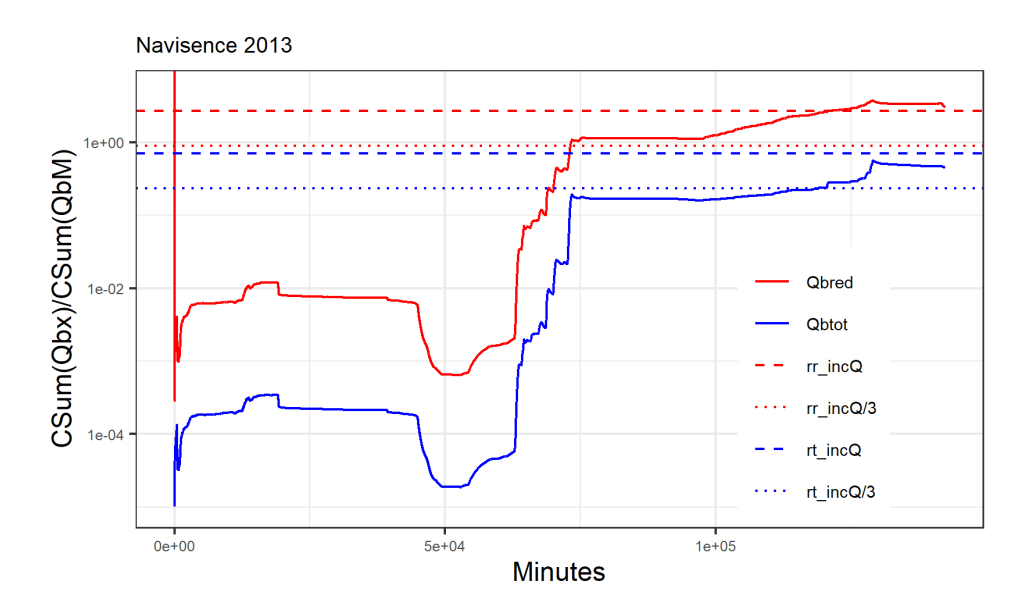
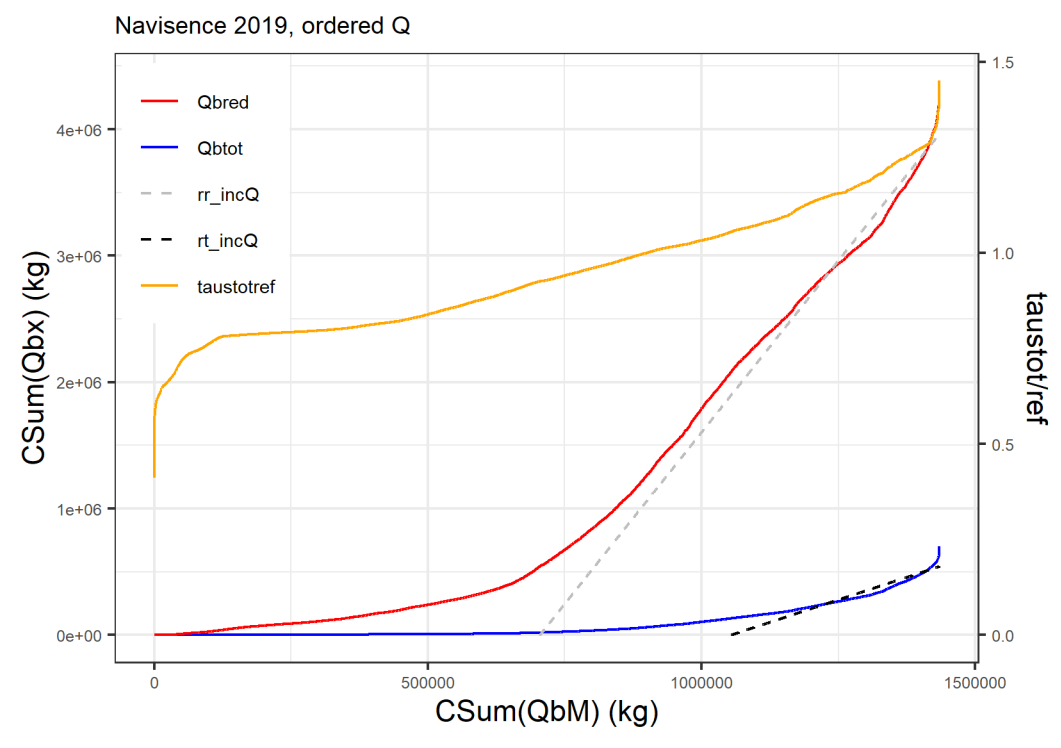


Figure S16. Navisence, summer 2013. (a) Application of a liner model (gray and black dashed lines) for the cumulative sum of calculated (SumQbx) vs. measured (SumQbM) bedload masses; values are ordered according to increasing discharge Q. (b) Ratio of cumulative sum of calculated (CSum(Qbx)) to cumulative sum of observed (CSum(QbM)) bedload masses vs. time (in minutes); values are in chronological order.



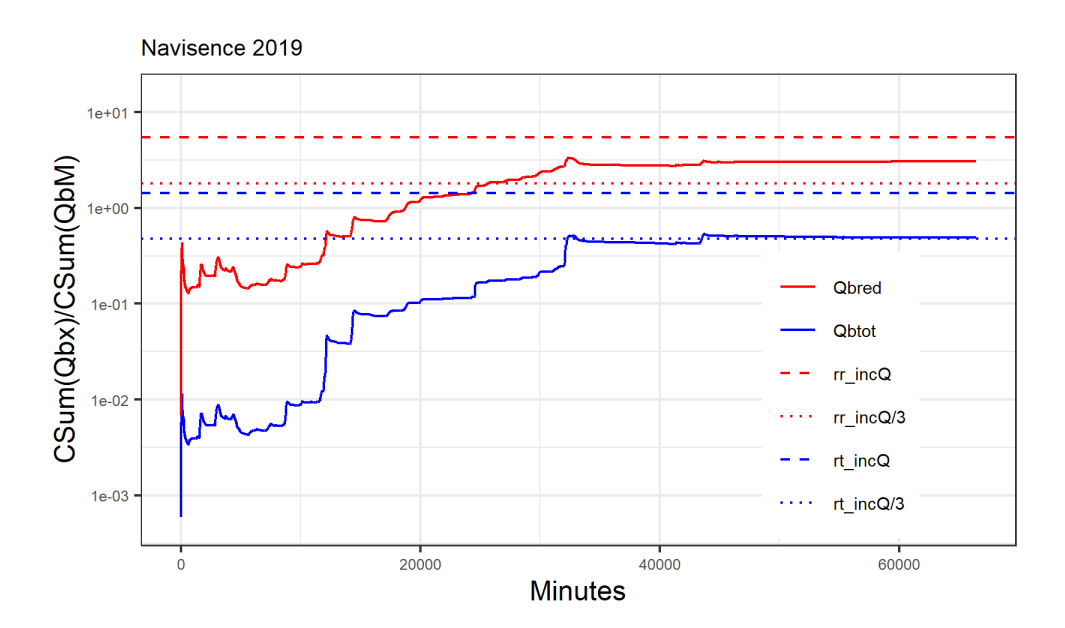
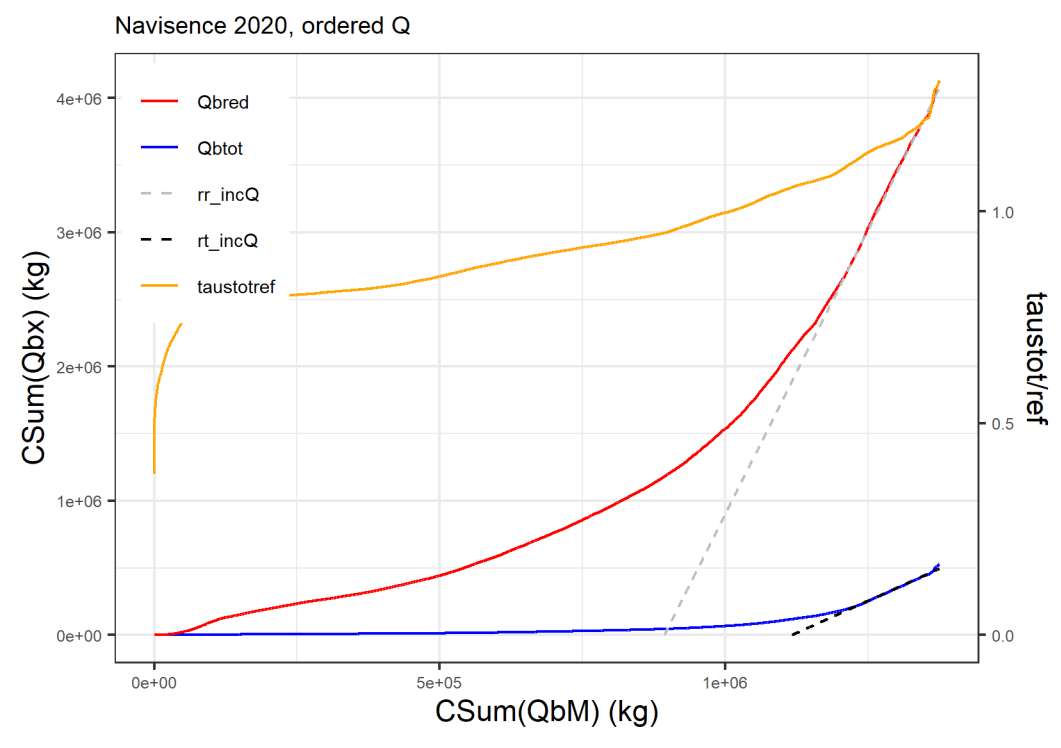


Figure S17. Navisence, summer 2019. (a) Application of a liner model (gray and black dashed lines) for the cumulative sum of calculated (SumQbx) vs. measured (SumQbM) bedload masses; values are ordered according to increasing discharge Q. (b) Ratio of cumulative sum of calculated (CSum(Qbx)) to cumulative sum of observed (CSum(QbM)) bedload masses vs. time (in minutes); values are in chronological order.



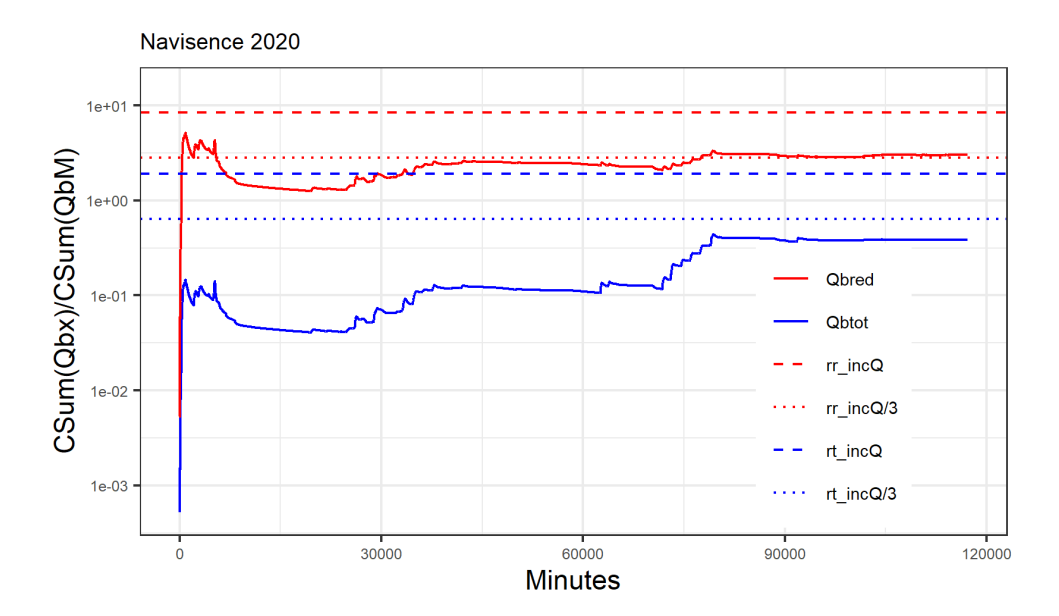
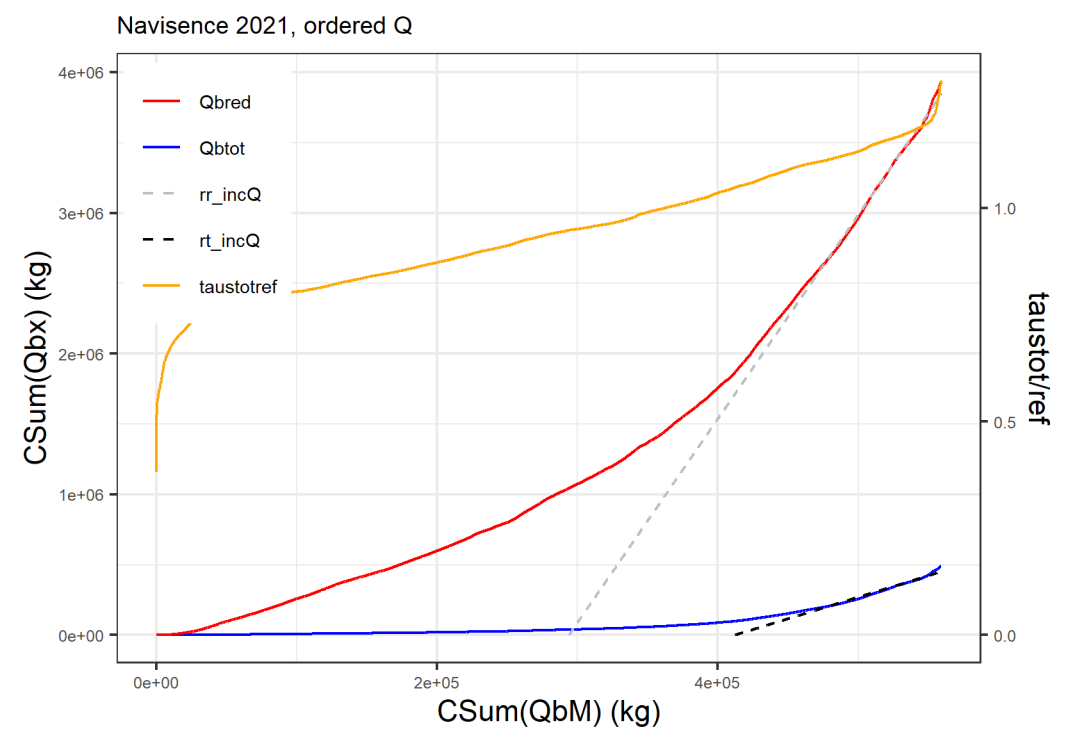


Figure S18. Navisence, summer 2020. (a) Application of a liner model (gray and black dashed lines) for the cumulative sum of calculated (SumQbx) vs. measured (SumQbM) bedload masses; values are ordered according to increasing discharge Q. (b) Ratio of cumulative sum of calculated (CSum(Qbx)) to cumulative sum of observed (CSum(QbM)) bedload masses vs. time (in minutes); values are in chronological order.



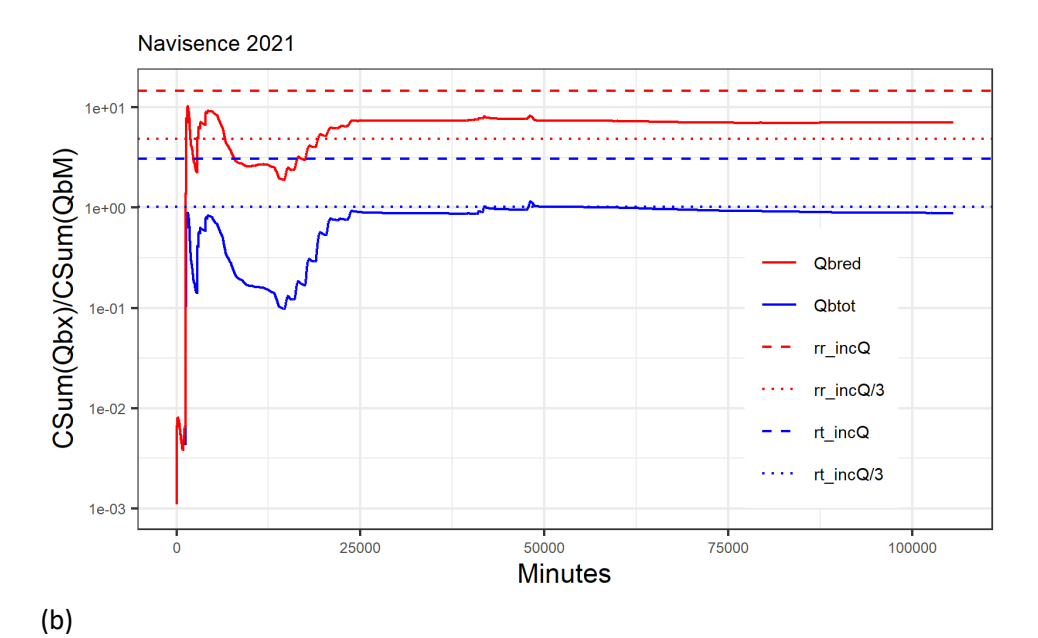


Figure S19. Navisence, summer 2021. (a) Application of a liner model (gray and black dashed lines) for the cumulative sum of calculated (SumQbx) vs. measured (SumQbM) bedload masses; values are ordered according to increasing discharge Q. (b) Ratio of cumulative sum of calculated (CSum(Qbx)) to cumulative sum of observed (CSum(QbM)) bedload masses vs. time (in minutes); values are in chronological order.

# $Q_b$ vs. Q plots for the Avançon de Nant

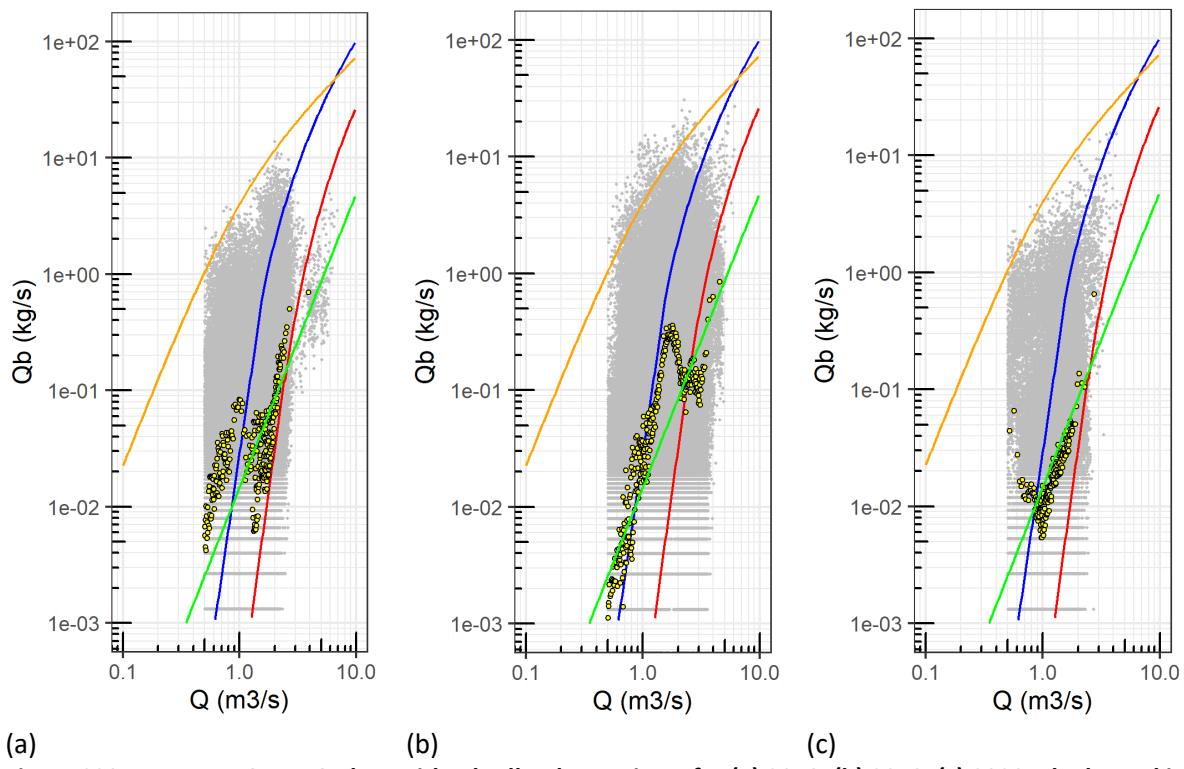


Figure S20. Avançon,  $Q_b$  vs. Q plots with 4 bedload equations, for (a) 2018, (b) 2019, (c) 2020. The legend is the same as in Figure 3 of the paper. The binned geometric mean values of  $Q_b$  for binned Q classes were determined by setting zero  $Q_b$  values to  $Q_b$  = 1e-5 kg/s, to match the  $Q_{bM\ binned}$  values for the Avancon 2019 in Figure 3.

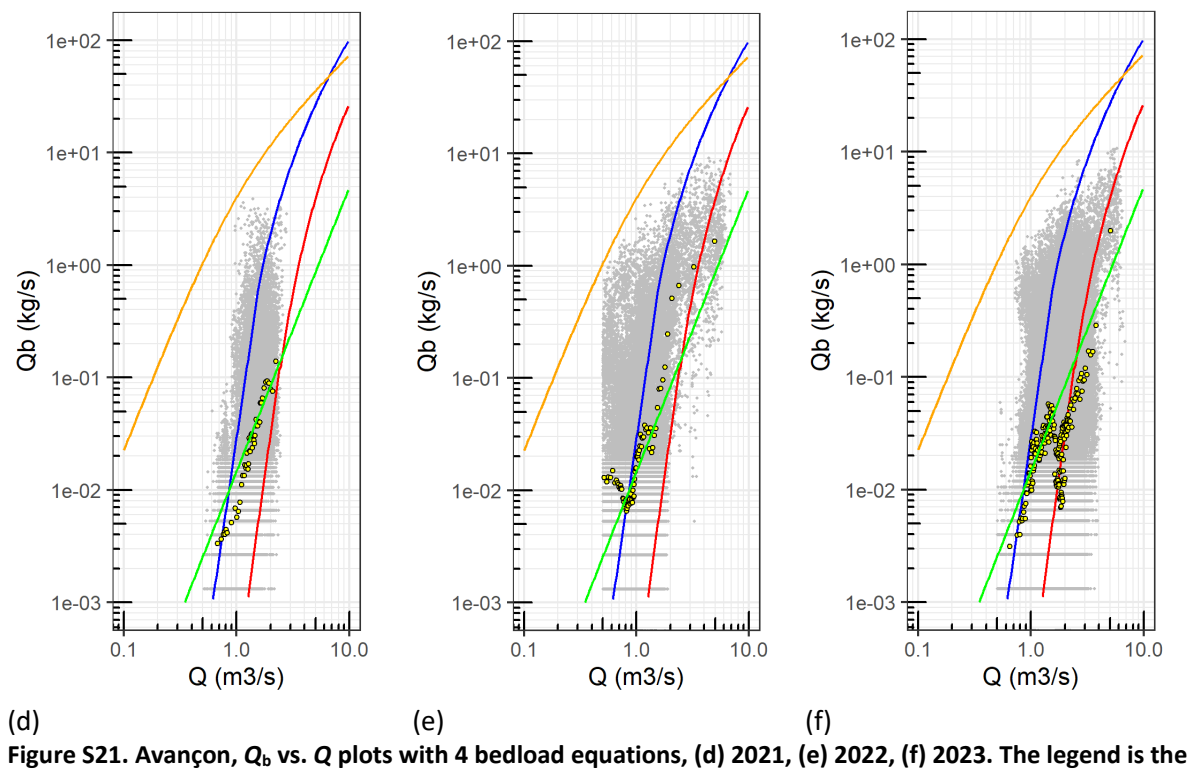
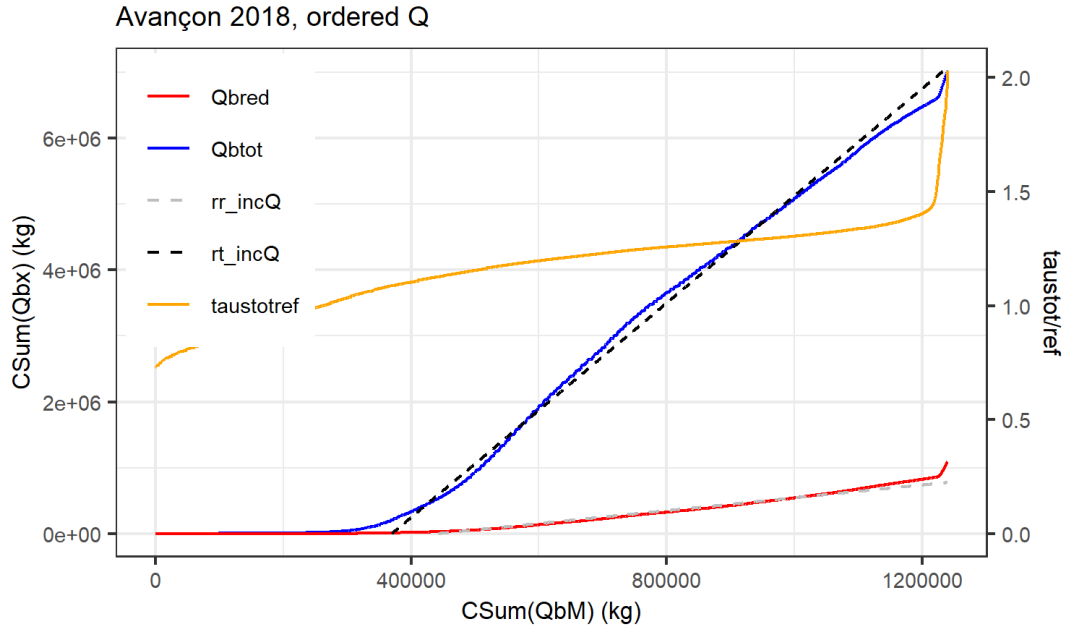


Figure S21. Avançon,  $Q_b$  vs. Q plots with 4 bedload equations, (d) 2021, (e) 2022, (f) 2023. The legend is the same as in Figure 3 of the paper. The binned geometric mean values of  $Q_b$  for binned Q classes were determined by setting zero  $Q_b$  values to  $Q_b$  = 1e-5 kg/s, to match the  $Q_{bM\ binned}$  values for the Avancon 2019 in Figure 3.

# CumSum analysis for the Avançon de Nant



(a)

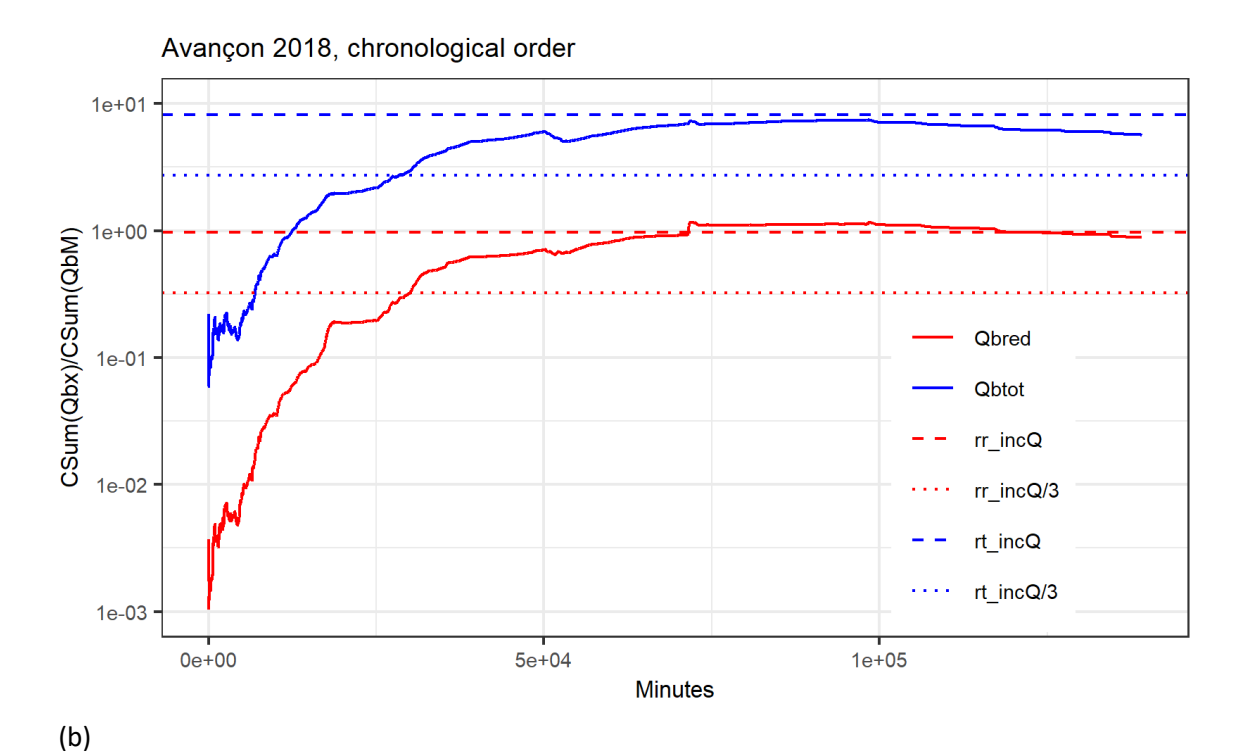
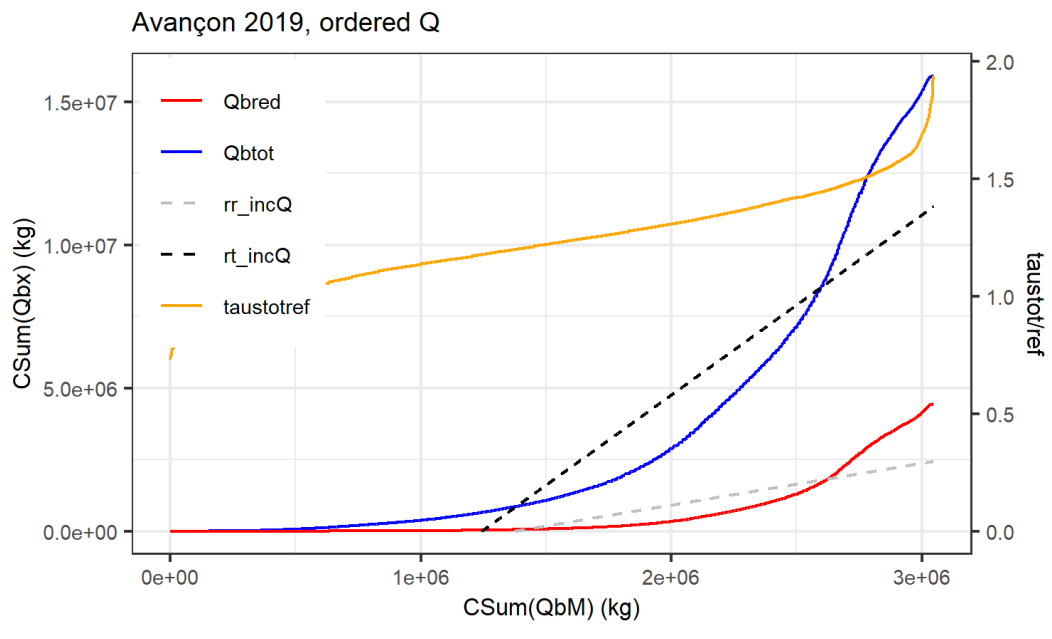


Figure S22. Avançon, summer 2018. (a) Application of a liner model (gray and black dashed lines) for the cumulative sum of calculated (SumQbx) vs. measured (SumQbM) bedload masses; values are ordered according to increasing discharge Q. (b) Ratio of cumulative sum of calculated (CSum(Qbx)) to cumulative sum of observed (CSum(QbM)) bedload masses vs. time (in minutes); values are in chronological order.



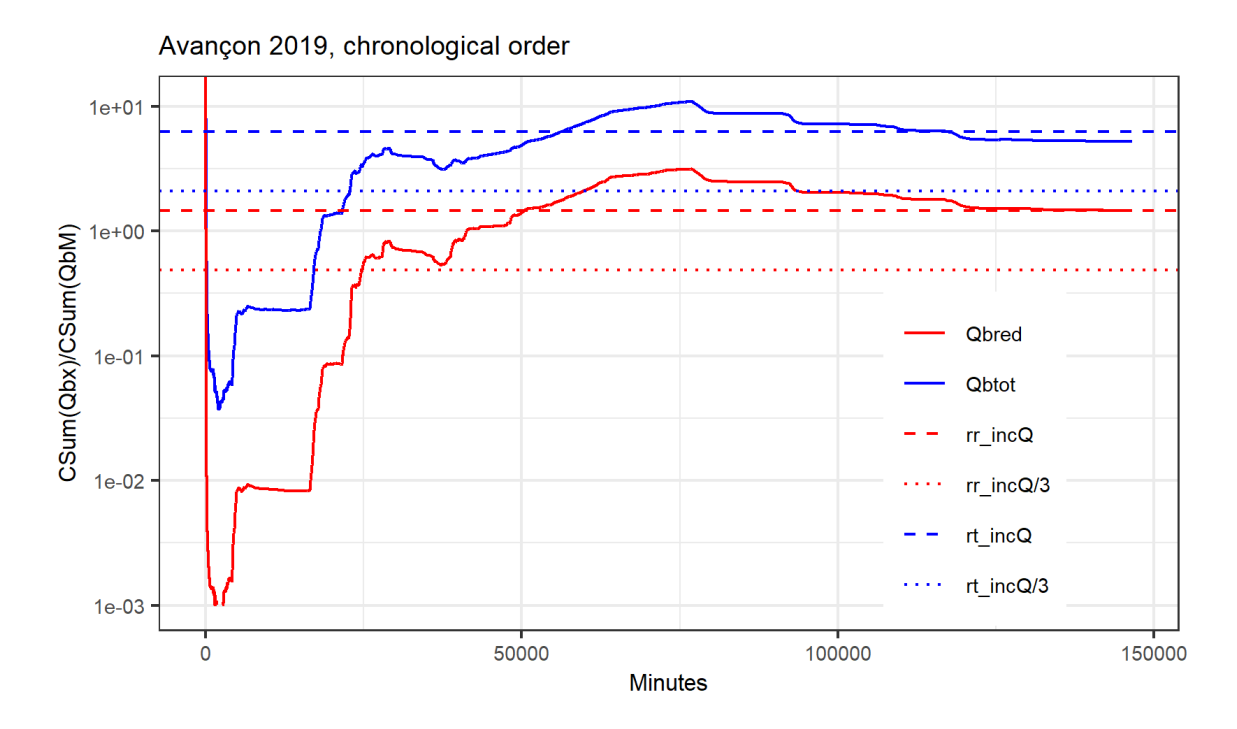
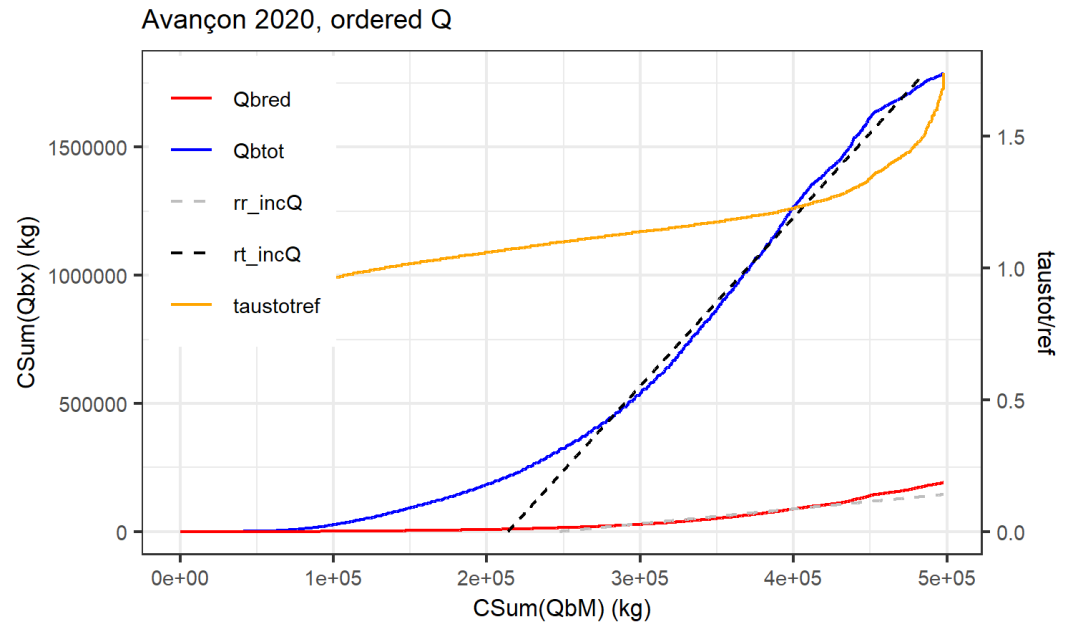


Figure S23. Avançon, summer 2019. (a) Application of a liner model (gray and black dashed lines) for the cumulative sum of calculated (SumQbx) vs. measured (SumQbM) bedload masses; values are ordered according to increasing discharge Q. (b) Ratio of cumulative sum of calculated (CSum(Qbx)) to cumulative sum of observed (CSum(QbM)) bedload masses vs. time (in minutes); values are in chronological order.



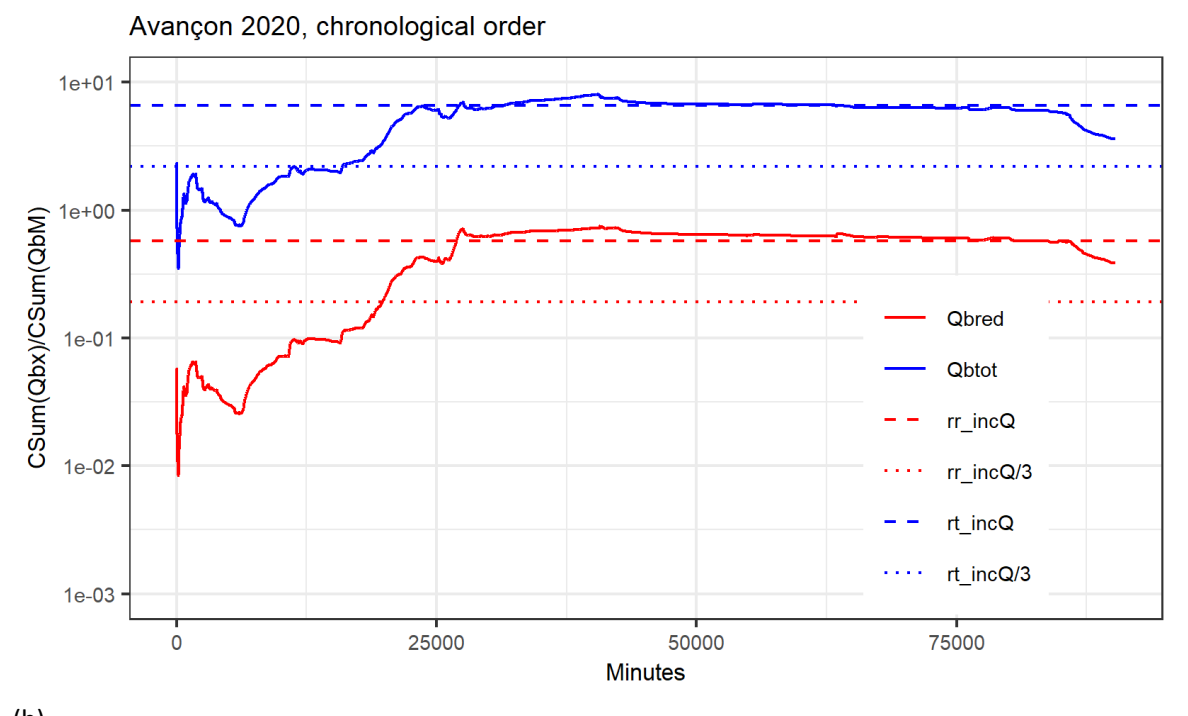
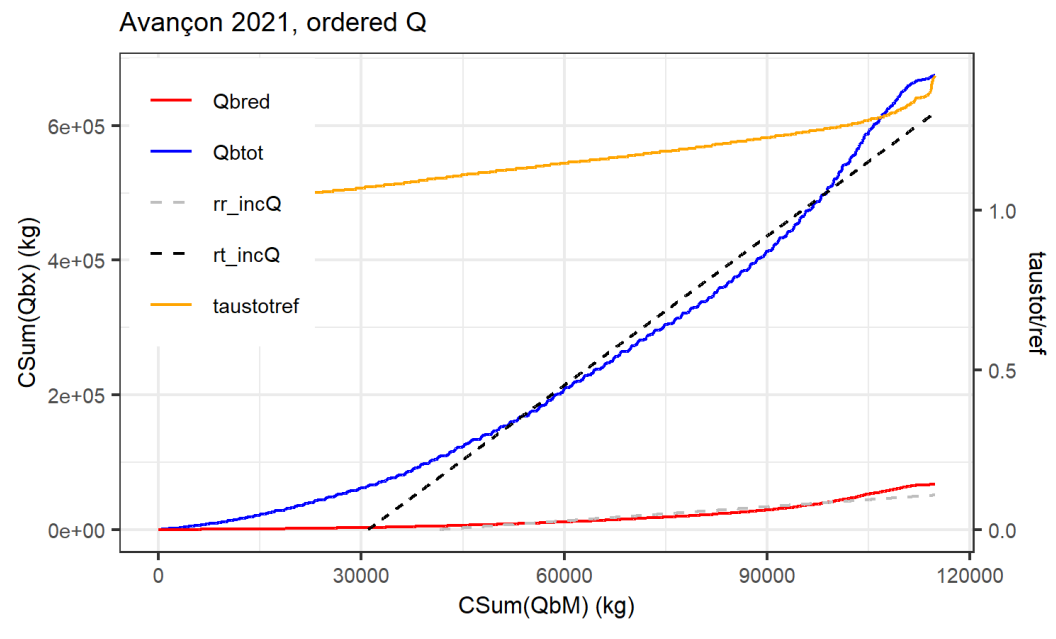


Figure S24. Avançon, summer 2020. (a) Application of a liner model (gray and black dashed lines) for the cumulative sum of calculated (SumQbx) vs. measured (SumQbM) bedload masses; values are ordered according to increasing discharge Q. (b) Ratio of cumulative sum of calculated (CSum(Qbx)) to cumulative sum of observed (CSum(QbM)) bedload masses vs. time (in minutes); values are in chronological order.



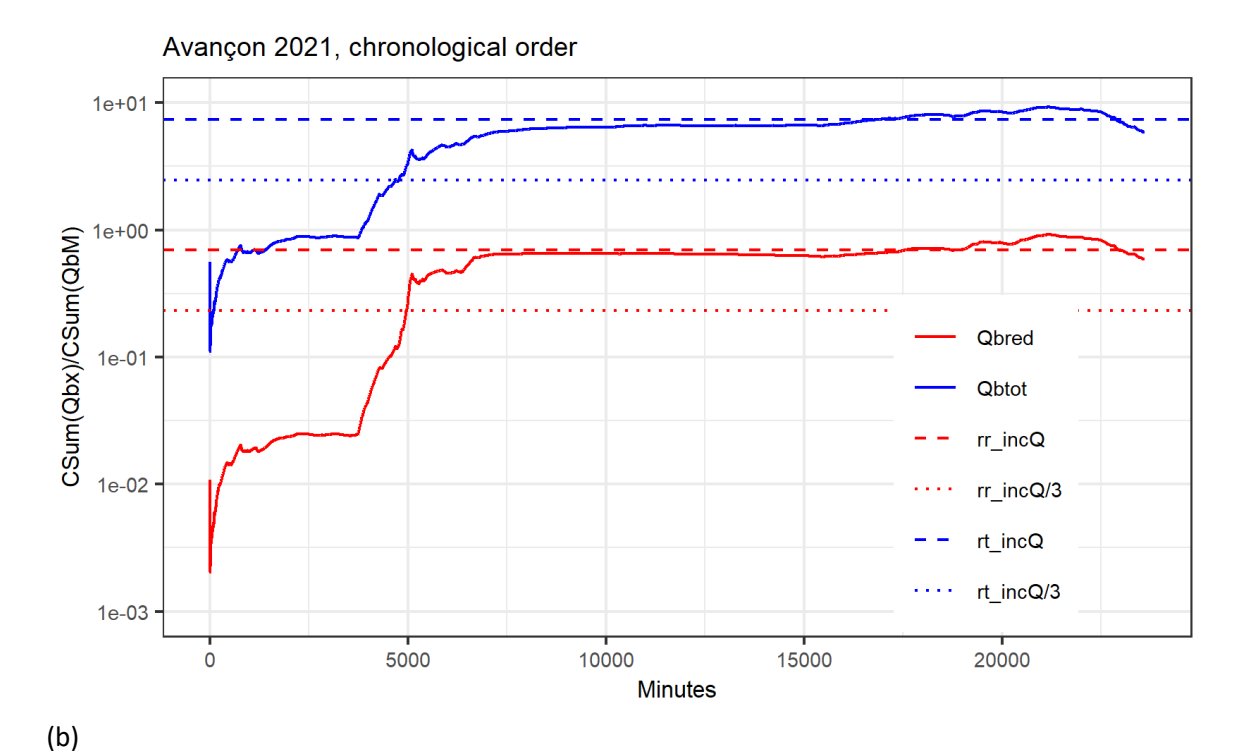
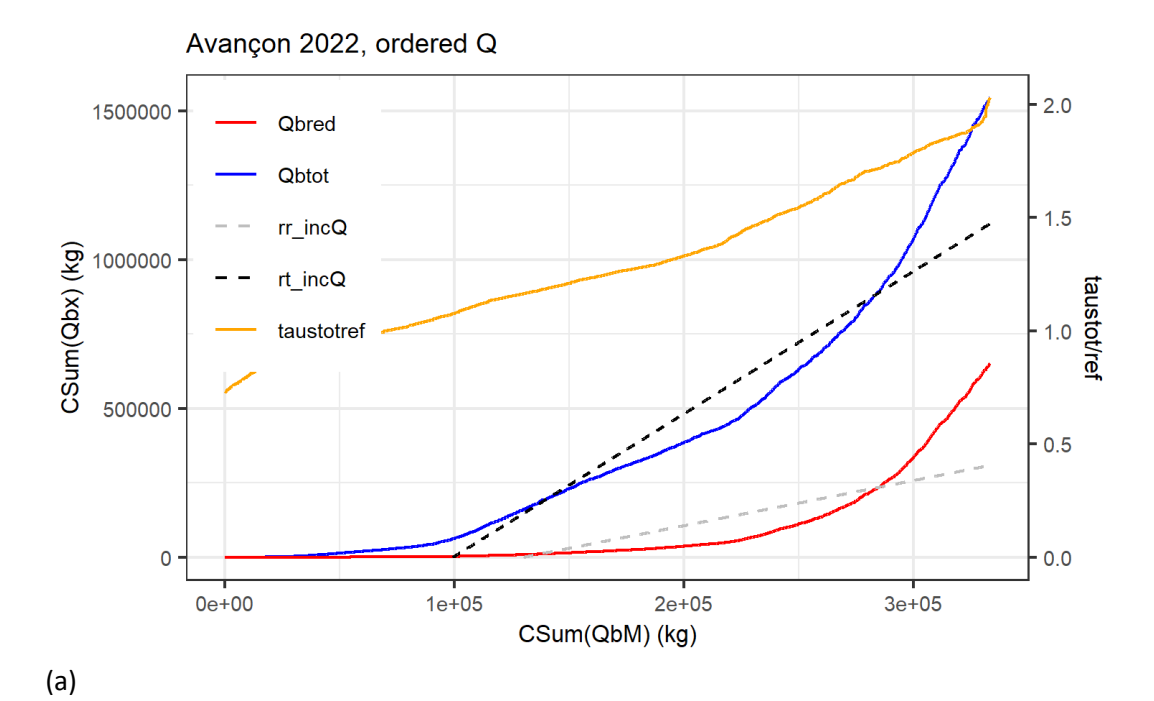
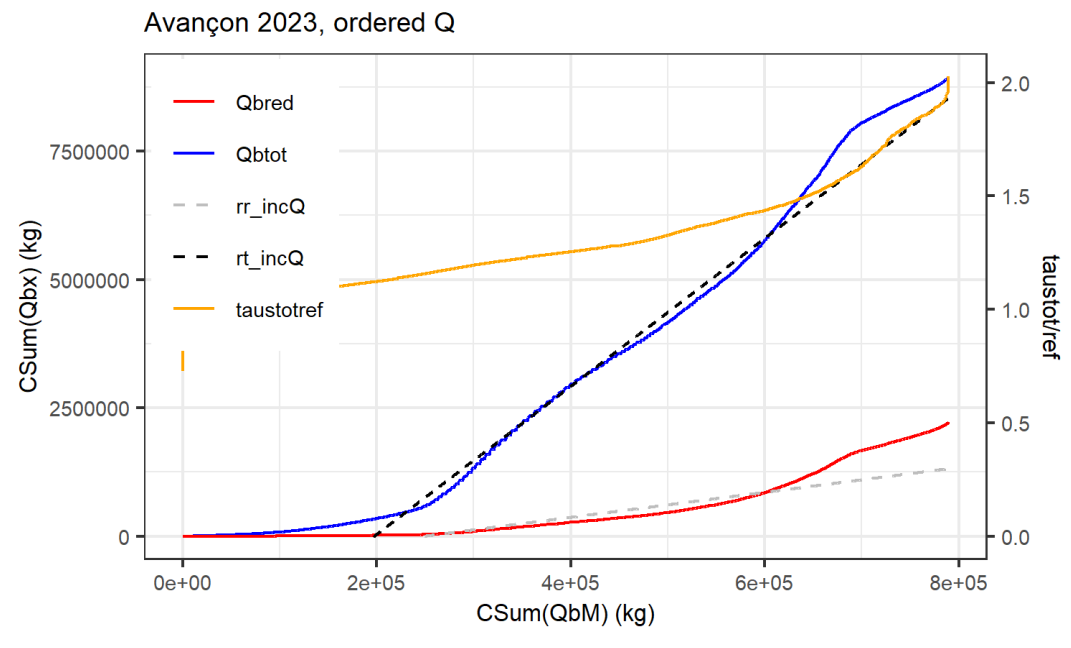


Figure S25. Avançon, summer 2021. (a) Application of a liner model (gray and black dashed lines) for the cumulative sum of calculated (SumQbx) vs. measured (SumQbM) bedload masses; values are ordered according to increasing discharge Q. (b) Ratio of cumulative sum of calculated (CSum(Qbx)) to cumulative sum of observed (CSum(QbM)) bedload masses vs. time (in minutes); values are in chronological order.



Avançon 2022, chronological order 1e+01 1e+00 CSum(Qbx)/CSum(QbM) Qbred 1e-01 Qbtot rr\_incQ 1e-02 rr\_incQ/3 rt\_incQ rt\_incQ/3 1e-03 10000 30000 20000 Minutes

Figure S26. Avançon, summer 2022. (a) Application of a liner model (gray and black dashed lines) for the cumulative sum of calculated (SumQbx) vs. measured (SumQbM) bedload masses; values are ordered according to increasing discharge Q. (b) Ratio of cumulative sum of calculated (CSum(Qbx)) to cumulative sum of observed (CSum(QbM)) bedload masses vs. time (in minutes); values are in chronological order.



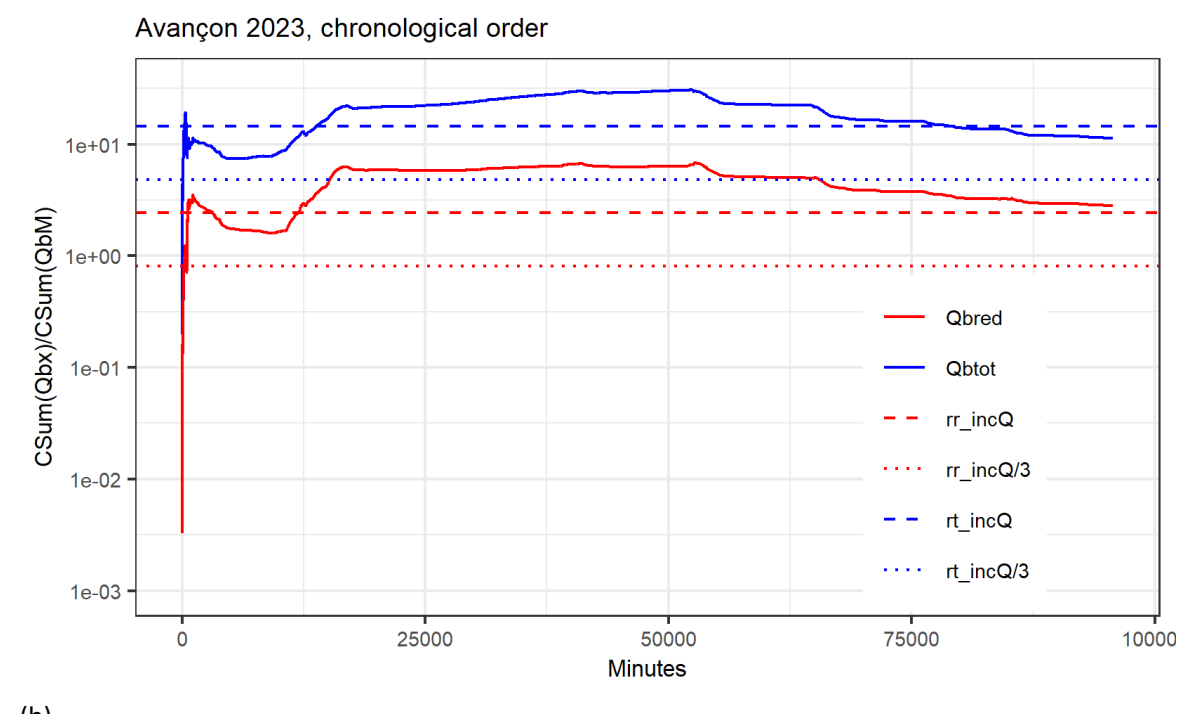


Figure S27. Avançon, summer 2023. (a) Application of a liner model (gray and black dashed lines) for the cumulative sum of calculated (SumQbx) vs. measured (SumQbM) bedload masses; values are ordered according to increasing discharge Q. (b) Ratio of cumulative sum of calculated (CSum(Qbx)) to cumulative sum of observed (CSum(QbM)) bedload masses vs. time (in minutes); values are in chronological order.

# $Q_b$ vs. Q plots for the Erlenbach

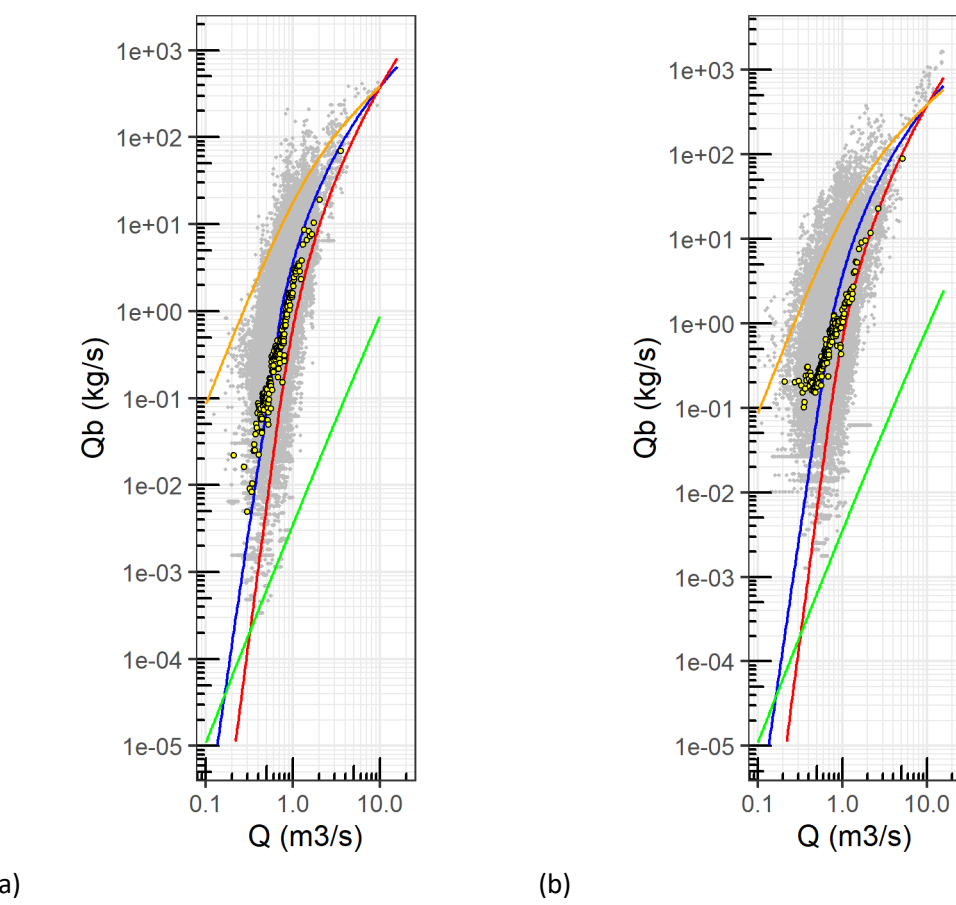


Figure S28. Erlenbach,  $Q_b$  vs. Q plots with 4 bedload equations, for (a) 1986-1999 (period A), and (b) 2012-2016 (period B). The legend is the same as in Figure 3 of the paper.

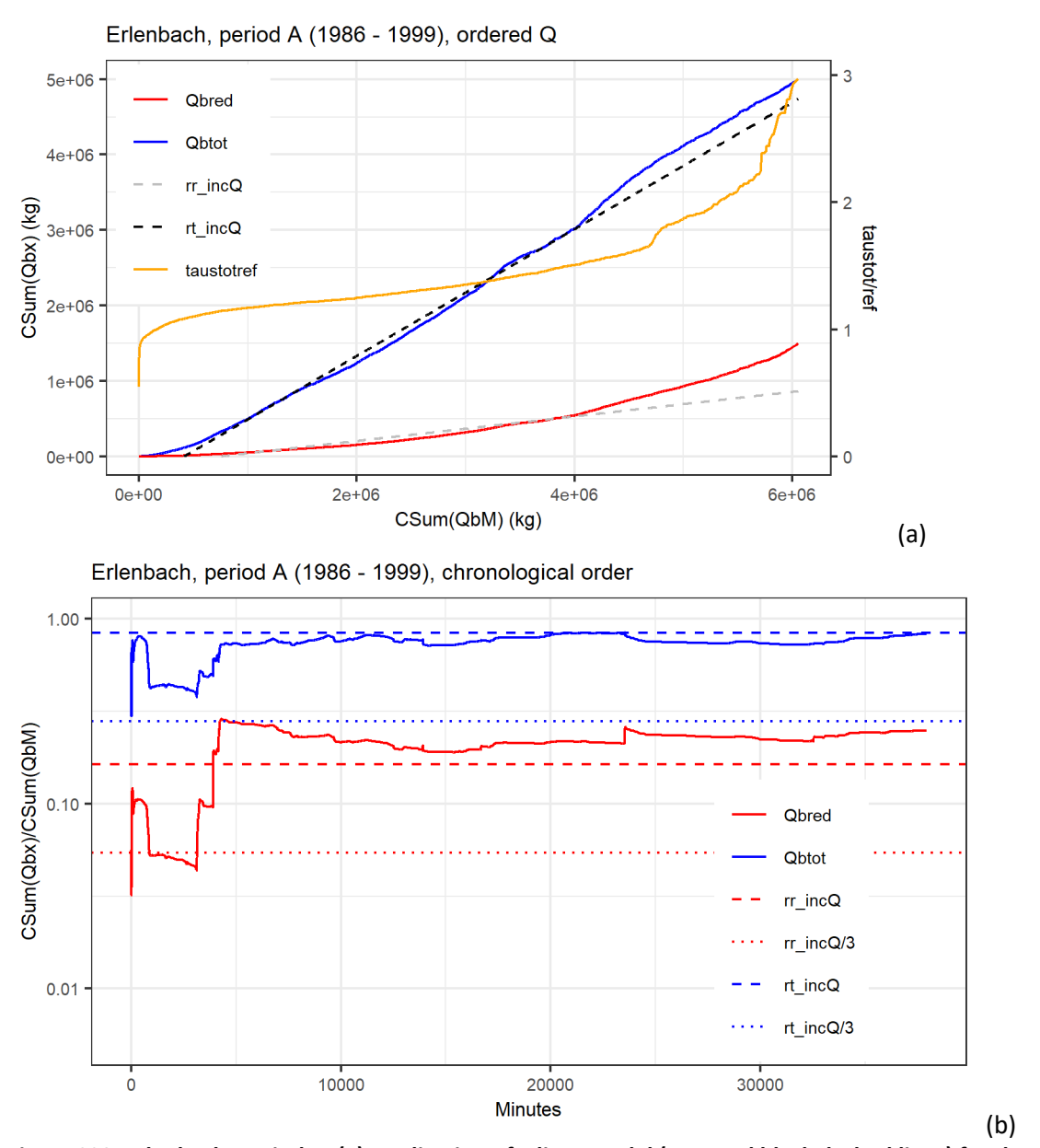


Figure S29. Erlenbach, period A. (a) Application of a liner model (gray and black dashed lines) for the cumulative sum of calculated (SumQbx) vs. measured (SumQbM) bedload masses; values are ordered according to increasing discharge Q. (b) Ratio of cumulative sum of calculated (CSum(Qbx)) to cumulative sum of observed (CSum(QbM)) bedload masses vs. time (in minutes); values are in chronological order.

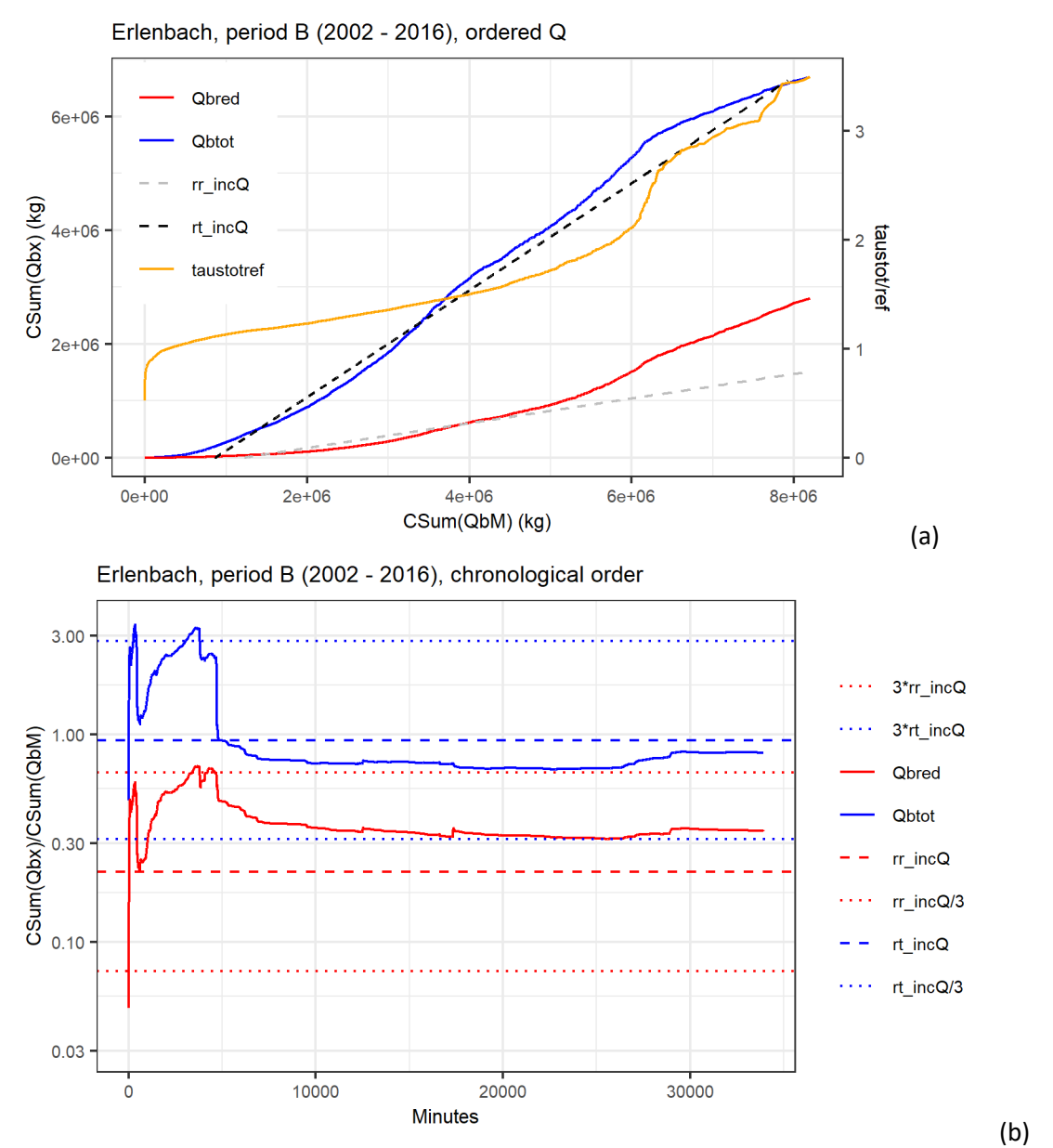


Figure S30. Erlenbach, period B. (a) Application of a liner model (gray and black dashed lines) for the cumulative sum of calculated (SumQbx) vs. measured (SumQbM) bedload masses; values are ordered according to increasing discharge Q. (b) Ratio of cumulative sum of calculated (CSum(Qbx)) to cumulative sum of observed (CSum(QbM)) bedload masses vs. time (in minutes); values are in chronological order.

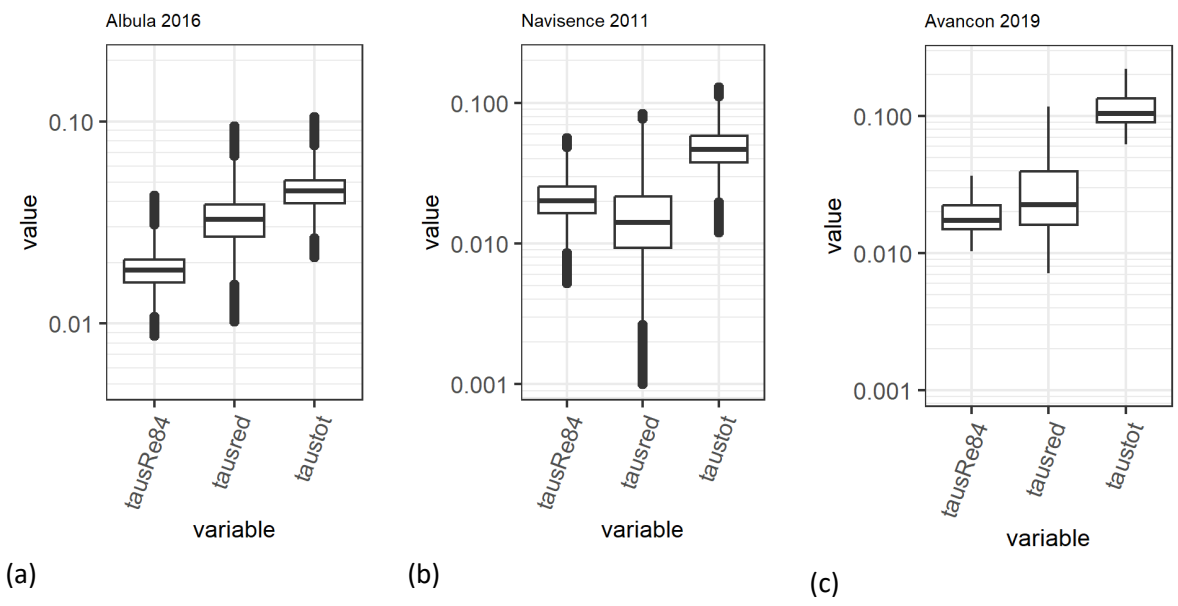


Figure S31. Boxplots of tausRe84 ( $\tau*_{Re84}$ ), tausred ( $\tau*_{D50}$ ), taustot ( $\tau*_{D50}$ ), for (a) Albula 2016, (b) Navisence 2011, (c) Avançon 2019.

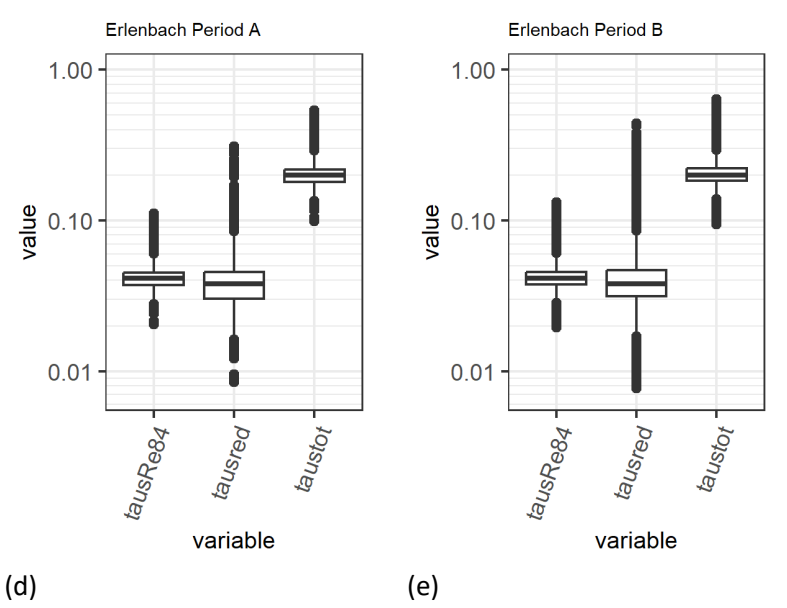


Figure S31\_contd. Boxplots of tausRe84 ( $\tau*_{Re84}$ ), tausred ( $\tau*_{D50}$ ), taustot ( $\tau*_{D50}$ ), for (d) Erlenbach Period A, (e) Erlenbach Period B.